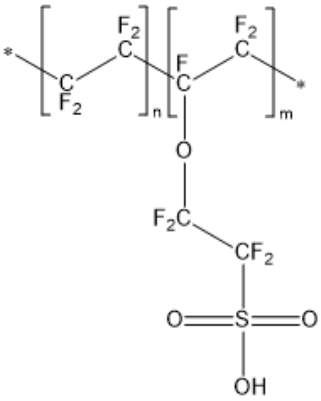

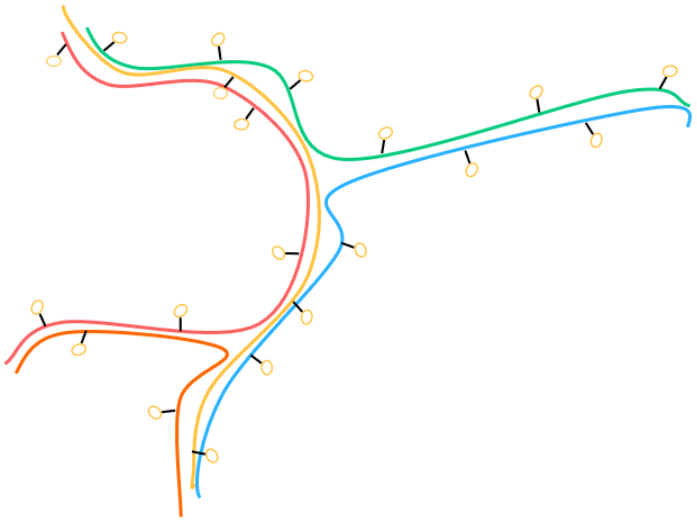

Rheological behavior of ionomer dispersions and their incorporation in catalytic inks for use in PEMFC electrodes

Master's thesis in Materials Chemistry

NORA MALMQUIST

DEPARTMENT OF PHYSICS

CHALMERS UNIVERSITY OF TECHNOLOGY
Gothenburg, Sweden 2023
www.chalmers.se

Master's thesis 2023

Rheological behavior of ionomer dispersions and their incorporation in catalytic inks for use in PEMFC electrodes

NORA MALMQUIST

CHALMERS
UNIVERSITY OF TECHNOLOGY

Department of Physics
Division of Chemical Physics
Chalmers University of Technology
Gothenburg, Sweden 2023

Rheological behavior of ionomer dispersions and their incorporation in catalytic inks for use in PEMFC electrodes
NORA MALMQUIST

Supervisor: Felix Ernst, PowerCell Group AB
Examiner: Björn Wickman, Department of Physics

Master's Thesis 2023
Department of Physics
Division of Chemical Physics
Chalmers University of Technology
SE-412 96 Gothenburg
Telephone +46 31 772 1000

Cover: Chemical structure of short side chain Perfluorinated sulfonic-acid ionomer (left) and structure of highly interconnected ionomer bundle (right).

Typeset in LaTeX
Printed by Chalmers Reproservice
Gothenburg, Sweden 2023

Rheological behavior of ionomer dispersions and their incorporation in catalytic inks for use in PEMFC electrodes
NORA MALMQUIST
Department of Physics
Chalmers University of Technology

Abstract

Proton exchange membrane fuel cells produce greenhouse gas emission-free electricity which is needed in the ongoing climate crisis. At the center of the fuel cell is a proton exchange membrane sandwiched between two electrodes produced from a catalytic ink. The ionomer component in catalytic inks acts both as a binder and a proton conductor and is an integral part of the catalyst layer. It is therefore important to have a thorough understanding of its key characteristics to optimize inks for improved processing and electrode performance and durability. Various perfluorinated sulfonic-acid (PFSA) ionomer dispersions with varying solvent matrices and ionomer amounts were mixed and their viscosity was tested before and after elevated temperature treatment as it is known to support the dispersion process of specific ionomers in solvent matrices. Only short-side chained and low equivalent weight ionomers showed significant change in viscosity. Higher alcohol concentrations as well as more sterically hindering alcohols in the solvent matrix lead to more thickening. Higher ionomer concentrations, higher temperatures, and longer heating times also lead to thicker dispersions up to a maximum viscosity where it is fully gelled. The influence of ionomer viscosity on ink mixing and dispersion was described as well. Heating catalytic inks with short-side chained PFSA ionomers thickens the ink but the resulting electrode decals are full of holes. Inks made by mixing pre-thickened ionomer with catalyst powder are difficult to mix and disperse properly. Using a more sterically hindering solvent will give a very thick ink even without any heating. The rheological properties of catalytic inks can be altered by changing the parameters that affect the structure of short-side chained and low equivalent weight PFSA ionomers but more investigation is needed into the dispersing of the inks as well as how altering of these parameters affect the resulting fuel cell performance. The increased understanding of the ionomer component will help to optimize the ink development and electrode design at PowerCell in the future which in turn will lead to more efficient fuel cells making them a more viable alternative to fossil fuel-based energy production.

Keywords: ionomer, fuel cells, perfluorinated sulfonic acid, solvent, PEM, catalytic ink, catalyst layer, rheology, viscosity.

Acknowledgements

I would like to thank my supervisor Felix Ernst for all of the support and guidance, as well as my examiner Björn Wickman. I also want to thank Marika Männikkö, Lorena Balint, Gabor Toth, Parinaz Mikaeli, Mats Larsson, and all of the other amazing colleagues at PowerCell for all the help and the warm welcome. A big thank you also goes out to Emma Ulberstad, Sandeep Jayaprakash Nair, Astrid Hjern, Xiaoling Jiang, Dylan Schulz, and Axel Lind for their help and company during the many hours in the lab. Finally, I would like to thank all of the other residents of Stöket for all of the laughs and good times we have had over the past few months.

Nora Malmquist, Gothenburg, May 2023

List of Acronyms

Below is the list of acronyms that have been used throughout this thesis listed in alphabetical order:

C/B	Cup and Bob
C/P	Cone-Plate
CCM	Catalyst Coated Membrane
CL	Catalyst Layer
ECSA	Electrochemical Surface Area
EtOH	Ethanol
EW	Equivalent Weight
HC	Hydrocarbon
HDPE	High Density Polyethylene
HOR	Hydrogen Oxidation Reaction
HSAC	High Surface Area Carbon
I/Pt	Ionomer to Platinum ratio
IEC	Ion Exchange Capacity
IPA	Isopropanol
LDPE	Low Density Polyethylene
LSC	Long-Side Chain
MEA	Membrane Electrode Assembly
MSC	Medium-side chain
NPA	N-Propanol
ORR	Oxygen Reduction Reaction
P/P	Plate-Plate
PEM	Proton Exchange Membrane *or* Polymer Electrolyte Membrane
PEMFC	Proton Exchange Membrane Fuel Cell *or* Polymer Electrolyte Membrane Fuel Cell
PFAS	Per- and Polyfluoroalkyl Substances
PFSA	Perfluorinated Sulfonic-Acid
Pt	Platinum
Pt/C	Platinum on Carbon support
PTFE	Polytetrafluoroethylene
RH	Relative Humidity
RS	Roller-Shaker

SSC	Short-Side Chain
sPPX-H^+	Sulfo-Phenylated Polyphenylenes
TB	Tert-butanol
US	Ultrasonicator

Contents

List of Figures

List of Tables

1
Introduction

The world's supply of fossil fuels is quickly running out and as climate change is constantly becoming a more threatening issue, we need alternative ways to produce energy. One way to do this is through fuel cells which produce electricity from chemical energy without combustion and can be used in stationary energy storage and production as well as in automotive, marine, and aviation applications. This means that fuel cells are in theory able to achieve a higher efficiency since they are not limited by Carnot efficiency. Depending on the fuel used, the only emission can be heat and water as opposed to greenhouse gases.

The first fuel cell was invented in 1839 by Welsh scientist Sir William Grove. He called it a *gaseous voltaic battery* as it produced electricity from hydrogen and oxygen [1, 2]. As interesting as his invention was, no one managed to make a practical device for over a century even as the theoretical understanding of the electrochemical principles grew. The English engineer Francis T. Bacon completed the construction of a working 5 kW fuel cell stack in 1952 and in the early 1960s, NASA used the first polymer electrolyte fuel cells for their Gemini Program developed by General Electric. The U.S. space program also used fuel cells for life support, guidance, and communications in the Apollo Program, and to this day, fuel cells are common in space programs [3].

There are several different types of fuel cells and they are defined by the electrolyte they use. There are alkaline fuel cells which use concentrated KOH, phosphoric acid fuel cells which use concentrated phosphoric acid, molten carbonate fuel cells which use a combination of alkali carbonates in a ceramic matrix, solid oxide fuel cells which use a nonporous metal oxide and finally proton exchange membrane fuel cells (PEMFC) which are the most common [3].

This thesis work is done in collaboration with PowerCell Group AB which works with proton exchange membrane fuel cells, sometimes called polymer electrolyte membrane fuel cells due to the electrolyte being composed of a proton-conducting polymer membrane. Different types of fuel cells use different fuels but PEMFCs use hydrogen and oxygen which it converts into water. They have high peak power density and operate over a wide range of ambient temperatures. There are no moving parts and the fuel cells are silent and last up to 20 000 hours according to PowerCell Group [4].

Fuel cells have been around for a long time but have until recent years been very

limited in use. There are several reasons for this, including relatively low efficiencies, the lack of hydrogen infrastructure, and the high cost of the system and its components. Expanding on hydrogen infrastructure is a massive undertaking but necessary for the future viability of fuel cells in day-to-day life. Another issue with hydrogen is that the majority of it today is produced from fossil fuels. This thesis does not deal with larger issues of hydrogen technology such as these but it is good to keep in mind that changes need to be applied both to the technology and to the infrastructure around it if we want our future to run on hydrogen. The low efficiency is more directly connected to the fuel cell system itself and a large part of the efficiency loss can be found in the core of the fuel cell, the membrane electrode assembly (MEA) in the form of Ohmic losses. MEAs also currently make up around 40 % of the cost of a fuel cell system which is why optimization of it is very important.

The focus for optimization is often on the utilization of the platinum catalyst found in the electrodes of the MEA or on reducing Ohmic losses in the membrane. The focus of this thesis is the effects of the ionomer binder in the catalyst layer which affects both the Pt utilization and the proton conduction. The ionomer is made of a proton conduction polymer similar to the membrane and it therefore affects the conduction of protons from the catalyst particle to the membrane. It also affects the flow of reaction gases and water to and from the catalyst and increases the mechanical stability of the catalyst layer and adhesion to the membrane. There are several types of ionomers which can vary both in their chemical composition and in their equivalent weight which measures the weight of polymer for each pendant acid chain. The morphology of the ionomer varies in different solvents. Heating the ionomer changes their rheological behavior in dispersions and inks, which in turn can influence the performance of the final electrodes.

1.1 Problem statement

The aim of this thesis is to gain knowledge about the ionomer behavior in PEMFC ink. Specifically, how the processing parameters such as the viscosity and viscoelastic behavior, and resulting electrode appearance and performance vary when using different solvent matrices for the ionomer, when heating the ionomer or ink, and when using different ionomers. This can in turn be used to optimize the fuel cell electrode performance in combination with studies of catalyst behavior and production techniques. Producing an optimal ink recipe is not the goal of this work. The goal is to build a solid knowledge base and a better understanding of ionomer behavior that can potentially be used for optimization in the future.

PowerCell does not produce in-house MEAs for use in their products at the moment and they currently only have the equipment for producing prototype MEAs. The findings of this thesis will be important for MEA R&D at PowerCell.

1.2 Demarcation

The focus of the thesis is the ionomer in the catalyst layer in the MEA and is not concerned with broader issues of fuel cell stacks and systems or with other parts of the MEA such as the membrane or gas diffusion layer. The thesis will also not deal with the effects of different coating or drying methods or from using different catalysts in the ink. No high oxygen permeability ionomers will be included nor any pore-forming agents. Good mixing and dispersion are of course needed to accurately measure and coat the ink and therefore some experiments and discussion will be dedicated to it. However, it is not the main focus and other effects that may arise from different levels of dispersion are not discussed.

2
Theory

2.1 Proton exchange membrane fuel cells

PEMFCs convert chemical energy to electrical energy in an MEA seen in Figure 2.1. The center of the MEA is a thin proton-conducting polymer electrolyte membrane (PEM) sandwiched in between two catalyst layers (CLs) called the catalyst coated membrane (CCM). On either side of the CCM, there is a gas diffusion layer (GDL) commonly made from carbon fiber paper or woven fibers which helps distribute the reaction gases. The CLs are also called electrodes and the one supplied with hydrogen gas is the anode and the one supplied with oxygen gas is the cathode. Oxygen is commonly supplied in the form of air [3].

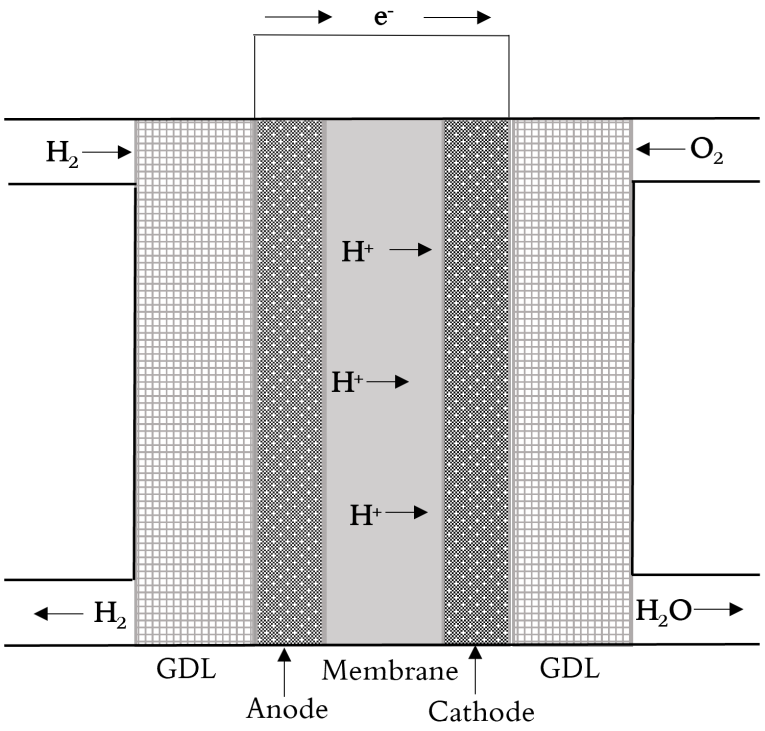

Figure 2.1: Schematic of a membrane electrode assembly of a proton exchange membrane fuel cell consisting of GDLs, an anode CL, a PEM, and a cathode CL.

The catalyst lowers the activation energy needed to oxidize hydrogen gas on the anode side of the MEA and the resulting electrons go into a circuit as an electri-

cal direct current while the protons are transported through the membrane to the cathode side where another catalyst layer reduces oxygen. Oxygen, protons, and electrons react to form water. The result is energy production that does not require any combustion or moving parts and emissions in the form of only water and warm air. The current is determined by the surface area of the MEA and the voltage by the number of cells. Each cell can theoretically generate a maximum of 1.23 V but in reality, they generate less than 1 V due to various losses. To produce significant voltages, several cells are stacked into what is called a fuel cell stack. A stack can contain hundreds of individual MEAs connected in series and separated by electrically conducting bipolar plates with flow channels that supply reaction gases and transport away the produced water [3, 5].

The reactions in a cell are:
HOR on Anode: $H_2 \longrightarrow 2\,H^+ + 2\,e^-$
ORR on Cathode: $\frac{1}{2}O_2 + 2\,H^+ + 2\,e^- \longrightarrow H_2O$
Total reaction: $\frac{1}{2}O_2 + H_2 \longrightarrow H_2O$

The oxygen reduction reaction (ORR) occurring in the cathode CL is often the rate-determining step as it has an exchange current density of $\sim 10^{-10}$ A/cm^2 compared to the much faster hydrogen oxidation reaction (HOR) in the anode which has an exchange current density of $\sim 10^{-3}$ A/cm^2 [6]. This means that the ORR is often the major cause of fuel cell power losses under load [7]. The cathode is also where the water is formed which makes it more prone to mass transport issues and flooding. The HOR is of course important too but due to the issues mentioned above, all electrodes prepared and discussed in this thesis will be prepared as cathodes.

2.2 Catalyst layer

The CLs of a PEMFC act as the electrodes of the electrochemical cell. The catalyst layer is composed of a noble metal catalyst, most commonly platinum (Pt) nanoparticles, on a mesoporous carbon black support with a proton-conducting polymer binder, called ionomer. The main component of the catalyst layer is the Pt catalyst on carbon support (Pt/C). The Pt particles generally have a particle size of 3 – 6 nm and the primary carbon particles are usually 15 – 30 nm in size but they tend to form aggregates with an average size of $\sim$ 100 nm to reduce their surface area [8]. Especially for cathodes, high surface area carbon (HSAC) is used which is very porous, with primary micropores (<2 nm) and mesopores (2 – 5 nm) on the particles. Secondary mesopores (5 – 50 nm) and macropores (>50 nm) can be found between the particles. The secondary pores are necessary for gas and water transport [9]. Anodes usually use more graphitized carbon supports which are more stable than HSAC but also have a lower surface area which results in lower reactivity due to a less even distribution of Pt particles. The catalyst aggregates are partially covered in an ultrathin ionomer film which serves both to provide structural integrity to the CL and transport protons to and from the membrane. The films are usually around 4 – 15 nm thick. The ultrathin films are mostly lamellar, and they are affected by the ionomer in dispersion before forming the electrodes. The size of dispersion

particles is strongly dependent on the solvent [10].

The microstructure of the CLs influences the electrochemical reactions in the fuel cell due to the varying triple-phase boundaries of the catalyst, the ionomer, and the reaction gas which is needed for the reaction to take place [7]. The CLs are porous and conduct electrons through interconnected catalyst, reaction gases through interconnected pores, and ions through interconnected ionomer [11]. During operation, there are various voltage losses and one of the major goals of electrode development is to minimize these. At very low currents, the electrochemical kinetics in the CL is responsible for sharp voltage drops, and at very high currents, voltage drops are associated with mass transport processes in the CL [6]. Significant quantities of water are produced via the ORR at high current densities, which need to be transported away to avoid flooding the pores. Ohmic losses can be observed in all current regimes and are typically attributed to protonic resistance in the ionomer in both the membrane and the catalyst layer [7].

Catalyst layers are typically 5 – 10 μm thick which leads to uneven reaction rate distributions due to gas and proton transport. This in turn leads to low utilization of Pt. Optimizing the use of Pt is another of the major goals of fuel cell research to make the technology more cost-effective. The incorporation of ion conduction polymers like PFSA in catalyst inks extends the three-dimensional reaction zone in the final CL which increases the utilization of the catalyst. By incorporating ionomers, Pt loadings can be decreased from several mg/cm^2 to <0.2 mg/cm^2 [8].

2.2.1 Catalytic ink

There are several ways of producing the CLs for PEMFCs which include decal transfer, spray coating, die coating, screen printing, and inkjet printing [12]. Most processes involve mixing a catalytic ink which is a colloidal dispersion composed of the Pt/C catalyst in the form of a powder, and the ionomer in a solvent matrix. The combined weight of the supported catalyst and ionomer is referred to as the solid content of the ink. The ratio between the ionomer and the Pt (I/Pt) is usually 0.7 – 1.3. Too high I/Pt can lead to too much water retention and swelling which clogs the pores and stops mass transport as well as isolation of the catalyst particles which lowers electron conductivity. Too low I/Pt can lead to not all Pt being in contact with the ionomer, reducing the amount of triple-phase boundaries where the reaction can take place which leads to lower electrochemical surface area (ECSA) and poor utilization of the catalyst [13]. The solvent matrix is usually a mixture of water and organic solvents. At PowerCell, water and various alcohols are used as solvents. PowerCell mainly uses a decal transfer procedure which uses ink with solid contents around 10 – 15 wt%. Inks optimized either for anodes or cathodes are coated on a carrier material using a doctor blade and allowed to dry to form the electrodes which are used to assemble the finished MEAs.

The heterogeneous microstructure of the ink strongly affects the structure and properties of the final catalyst layer. The solvent matrix which acts as a dispersing agent

interacts with both ionomer and catalyst and governs properties like particle aggregation size, ionomer aggregate size, viscosity, drying rate, and finally the solid microstructure of the CL which affects its physical and mass transport properties [7, 12]. Alcohols are commonly used as part of the solvent matrix due to them being relatively easy and safe to work with compared to other organic solvents. CLs made with alcohol-based solvent matrices also tend to perform better and the decals have smoother surfaces [14]. The organic solvent is needed to properly wet the hydrophobic carbon support and ionomer backbone. Higher proportions of water in the solvent matrix lead to larger ionomer aggregates and a lower radius of gyration [12]. Inks with only water used as the dispersing agent tends to form CL with lower ECSA than ones with alcohol due to better ionomer dissolution and higher functional group availability leading to better utilization of the catalyst [15]. Isopropyl alcohol is often used in catalytic inks but efforts are being made to avoid it due to concerns of dehydrogenation of IPA into acetone over the Pt catalyst [16]. Acetone is not a suitable solvent for catalytic inks as its low boiling point leads to very fast evaporation which causes cracking in the CL [14]. The ionomer and the catalyst particles form heterogeneous structures independently in solution before mixing and the final morphology of the CL is in large part affected by the structure of the individual components. As the deposited ink dries, ionomer concentration increases and polymer chains form independent rods and micelles intercalate with each other and the catalyst aggregates which provide mechanical strength to the CL.

The dispersion step is also an important part of ink preparation. To keep the size of the catalyst agglomerates as small as possible, dispersion methods such as ball milling or sonication are commonly used [17].

2.3 Perfluorinated sulfonic-acid ionomers

Ionomers play an important role in PEMFC since they make up both the membrane and the binder in the catalyst layer. They need to be stable enough to withstand the aggressive, oxidizing environment of an operating fuel cell [5]. Perfluorinated sulfonic acid (PFSA) ionomers are the most common type used in PEMFCs. They are chemically and mechanically very stable and they have very low gas permeability as well as being proton-conducting and electrically insulating. PFSA is a thermoplastic random copolymer with a semicrystalline polytetrafluoroethylene (PTFE) backbone which provides mechanical stability and perfluorovinyl ether side chains ending in sulfonate groups which can be ionized to sulfonic acid groups in the presence of water that transport protons [18]. There is a micro-phase separation between the hydrophobic backbone and the hydrophilic side chains forming nano-domains of a few nanometers [19]. An important parameter of ionomers is their equivalent weight (EW) which is defined as the weight of dry ionomer per mole of sulfonic acid groups. EW is inversely proportional to the ion exchange capacity (IEC) and depends on both side chain length and backbone length between each side chain as seen in Equation 2.1 where n is the backbone length. The backbone needs to have a sufficient number of tetrafluoroethylene monomers, usually $n \geq 4$, in order to crystallize, meaning that ionomers with longer side chains generally need a higher

EW than ionomers with shorter side chains to be useful in fuel cells [5].

$$EW = \frac{g_{polymer}}{mol_{SO_3}} = \frac{1000}{IEC} = 100n + MW_{side-chain} \tag{2.1}$$

The first commercial PFSA ionomers were long-side chain (LSC) ionomers and they are still very common. In recent years, short-side chain (SSC) ionomers have gained more interest due to better proton conduction in devices, higher glass transition temperatures, and better mechanical stability at lower EWs as a result of the absence of a -CF_3 pendant chain and the shorter side chain [20, 21]. They have also been shown to exhibit better polarization performance and higher voltage output in in-situ tests at higher temperatures and lower relative humidity [22]. SSC ionomer can have better Pt utilization and effectiveness in CL due to better accessibility of the ionomer to the carbon surface and Pt as a result of a more continuous coverage [21]. Figure 2.2 shows the chemical structure of an LSC and an SSC ionomer. The side chain length can be a useful tool for distinguishing between different ionomers but it is a relative measure and there are ionomers with side chain lengths between the archetypal LSCs and what is normally referred to as SSCs. For simplicity, those ionomers will be referred to as medium side chain (MSC) ionomers in this work and they look similar to SSC but with more -CF_2- segments. Only one is used in this study and it has 4 -CF_2- segments. The side chain chemistry affects the material properties as well as the length and therefore also has to be considered. SSC and MSC lack the fluoroether group that LSC has which makes the SSC and MSC polymer chains less prone to "unzipping" or degrading in a radical attack [23, 24].

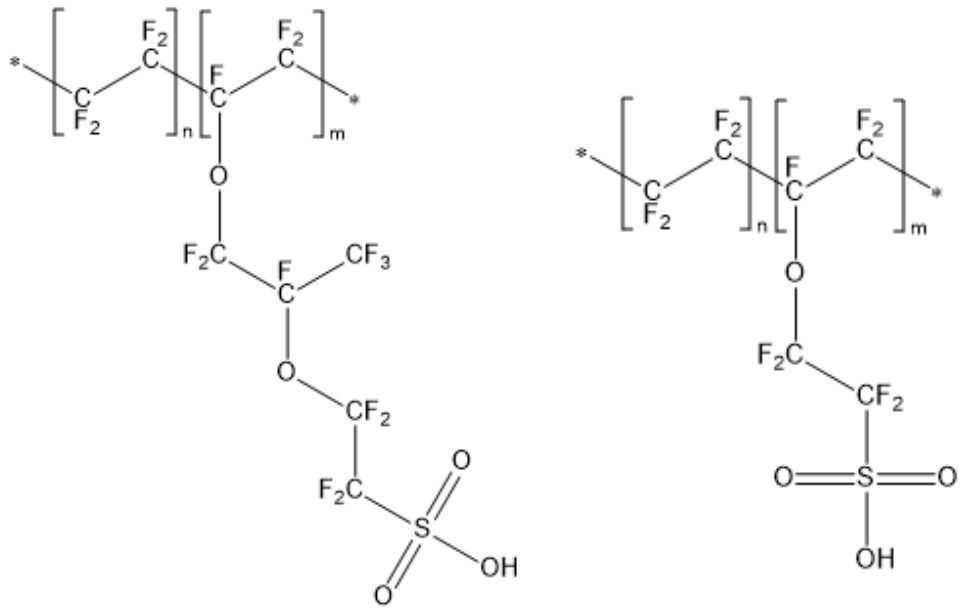

Figure 2.2: Chemical structure of LSC PFSA ionomer (left) and SSC PFSA ionomer (right). Varying n and m alter the EW of the ionomer.

PFSAs do not form true solutions in aqueous and alcoholic solvents but instead show a dispersion-like behavior with rod-shaped aggregates [25, 26]. The structure

is governed both by the polarity of the solvent and the solubility of the backbone. In more polar solvents the backbone has lower solubility and will form a dense core of the aggregates while the ionic moieties sit at the polymer-solvent interface. The radius of the rod is 20 – 25 Å for LSC and 15 – 17 Å for SSC ionomers depending on the solvent. The lower radius of SSC rods is mostly due to the lower EW. A mixture of alcohol and water has better solubility of ionomers than pure water or pure alcohol and the ratio is important for the morphology of the ionomer aggregates and the amount of solvent penetrating it. Highly solvated large particles (>200 nm) are formed in the mixture which increases viscosity [27]. Mixes of ionomer and solvent are referred to as dispersions in this work.

In dilute dispersions, SSC ionomer forms multimolecular micelles with an estimated diameter of 30 – 60 nm with the sulfonated side chains pointing outwards (in polar solvents). In higher concentrations or in solvents that solubilize the ionomer very well, it forms interconnected bundles as seen in Figure 2.3 which leads to significantly higher viscosity and eventually irreversible gelling [21].

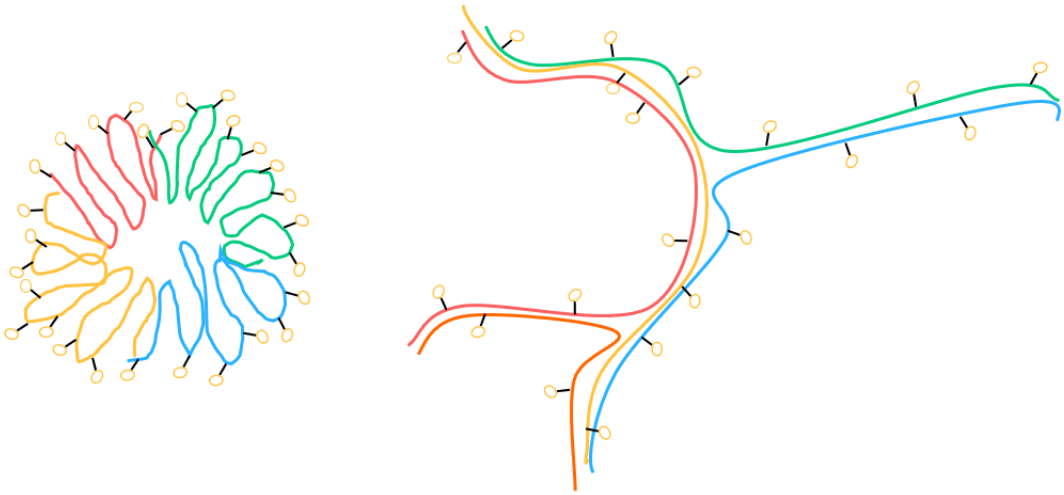

Figure 2.3: Multimolecular PFSA micelle (left) and interconnected bundles of PFSA (right) where the different colors represent different polymer chains and the black lines with yellow circles represent the ionomer side chains and the sulfonic acid group.

Another important factor is the sterical hindrance the solvent provides. A solvent that can solubilize the ionomer well, meaning interacting with both the hydrophobic backbone and hydrophilic side chains will be able to penetrate the ionomer micelle and cause interactions between different polymer chains and multimolecular bundles. Solvents that are more sterically hindering will prevent the tight micelle structures from reforming and thereby cause a viscosity increase in the dispersion. The solvent-dependent state of PFSA aggregates and their dispersion is still not fully understood and vary with EW, side chain chemistry, concentration, solvent matrix, and temperature making it a complex topic to study.

2.3.1 Issues with PFSA

Despite PFSA being the most common ion-conducting material for use in fuel cell MEAs, they are not without issues. PFSA ionomer in CLs complicates the recycling and reclamation of Pt. They also form hydrogen fluoride as a degradation product during fuel cell operation which is believed to promote the dissolution of Pt [7].

PFSA ionomers are classified as per- and poly-fluoroalkyl substances (PFAS). Several government agencies in the EU are working towards assessing and regulating PFAS as a group where the goal is to minimize and eventually end the use of PFAS since many PFAS are suspected of being harmful, bioaccumulate, and biomagnify and they are all very difficult to break down. There is limited knowledge of the health effects of many PFAS but according to the Swedish Chemical Agency, there is good reason to consider all PFAS as a health hazard [28]. In February 2023, the European Chemicals Agency published a restriction proposal for around 10 000 PFAS, including PFSA ionomers, submitted by authorities in Denmark, Germany, the Netherlands, Norway, and Sweden [29]. Chemical manufacturer 3M announced in a press release in December 2022 that they are to discontinue all PFAS manufacturing by the end of 2025 citing "the evolving external landscape, including multiple factors such as accelerating regulatory trends, focused on reducing or eliminating the presence of PFAS in the environment and changing stakeholder expectations" as the reason [30]. Other producers have revealed in interviews that they will continue their production with hopes of exemptions, but they will evaluate and alter their production procedures.

2.4 Hydrocarbon based ionomers

Due to the issues mentioned above, there has been a growing interest in replacing PFSA ionomers with hydrocarbon (HC) based ionomers in fuel cells. HC ionomers are not as well studied or commonly used in PEMFCs as PFSA but there have been a few studies where they seem promising for the future [31, 32]. HC-based polyaromatic and polyheterocyclic polymers can act as ionomers but they differ from PFSA ionomers in several ways. The sulfonic groups are often attached directly to the polymer backbone as opposed to on side chains which restrict the separation of the hydrophobic backbone from the hydrophilic acid group. This leads to a less pronounced phase segregation [6]. HC polymers are more tolerant of high temperatures which makes them good candidates for future high temp applications such as automotive.

There exist many different types of HC ionomers but the one used in this thesis work is a variation of sulfo-phenylated polyphenylenes (sPPX-H^+) with an IEC of 2.8 – 3.1 meq/g. X is an aryl group such as Phenyl (P), Biphenyl (B), or Naphthyl (N) [33]. The chemical structure can be seen in Figure 2.4 where Ar represents an aryl group. The exact structure is confidential.

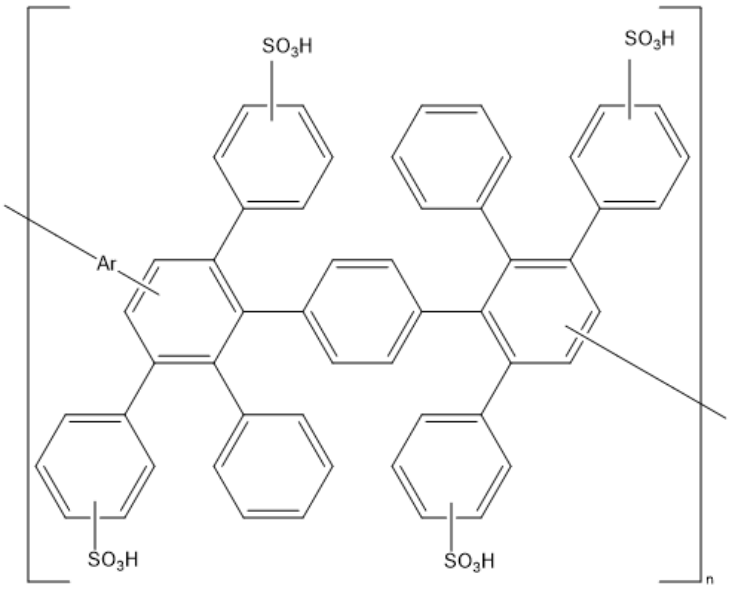

Figure 2.4: Chemical structure of sulfo-phenylated polyphenylenes. Ar represents an aryl group.

2.4.1 Issues with HC

Sulfonic acid groups on HC-based ionomers are weaker acids with a pK_a between -2 and -1 compared to PFSA with a pK_a of $\sim$ -6 [7]. HC ionomers also have a lower density than PFSA ionomers which combined with the lower pK_a means that HC ionomers often require more than twice the amounts of functional acid groups and consequently a higher IEC to achieve the same protonic conductivity as PFSA. This leads to higher hydrophilicity and more sensitivity to the hydration [32]. Low hydration causes brittleness and too high makes the ionomer too gelatinous [7].

In general, the optimal I/Pt of HC ionomers in CLs is lower than for PFSA. This lead to a slightly lower proton conductivity and lower ECSA in the CL which leads to a lower performance in the kinetic region despite similar peak power densities [32]. MEAs fully made of sPPX-H^+ as opposed to PFSA are more dependant on the humidity of the gas feed. The manufacturer of the HC ionomer used in this thesis has disclosed that this particular ionomer is unsuitable in cathodes due to poor oxygen solubility causing issues with reaction gas transport and that more appropriate variations are being developed. Low oxygen permeability is desirable for membrane materials but is detrimental to the cathode.

The normal decal transfer procedure and ink formulations used for PFSA-based catalytic inks are not appropriate when using HC ionomers. In an interview with the supplier, they recommended coating directly onto the membrane as opposed to on a separate PTFE decal carrier due to the repulsion between the ionomer and PTFE causing beading of the ink and poor adhesion to the carrier. The significantly higher glass transition temperature of the ionomer also means that the electrodes and membrane can not be thermally bonded together by hot pressing and instead

solvents are needed for the layers to combine properly. When coating directly on the membrane, less alcoholic solvent matrices and faster drying times are necessary to avoid dissolving the membrane. When changing any ink parameter, other properties like interactions between the solvent and catalyst, agglomeration behavior, and rheological properties among others also change. This means that entirely new optimizations of all stages of the manufacturing procedure have to be done when switching from PFSA to HC ionomers which also complicates any comparison between the ionomer types.

2.5 Rheology

The main method of characterizing differences between samples in this work is rheology. Rheology is the study of the flow and deformation of matter and it is a useful tool for characterizing material properties of fluids such as the catalytic ink used to produce the electrodes or ionomer dispersions. The tool used to study rheology is a rheometer in which the sample is placed between two plates (P/P), between a cone and a plate (C/P), or in a cup with a bob (C/B). The plate, cone, or bob, called the upper geometry rotates or oscillates to exert stresses on the sample which deforms it. The rheological properties of the ink are important to understand since they affect how the ink will behave during handling and coating and they can also indicate the microstructure of the ink and ionomer dispersion [17].

2.5.1 Rotating measurements

Rotating measurements can be used to characterize the viscosity of an ink. This is done by shear flow in which the layers of the ink slide past one another. An external shear force in the form of shear stress (σ) which is defined as the force (F) per unit area (A) as seen in Equation 2.2, is exerted on the sample and in response the top layer moves a given distance (x) while the bottom layer is stationary. The shear strain (γ) is defined in Equation 2.3 as the displacement gradient over the height (h). For a solid the strain will be infinite but for a fluid the shear strain will continue to increase for the period of applied stress which creates a velocity gradient called the shear rate ($\dot{\gamma}$) which is defined as the change of strain with time as seen in Equation 2.4. The shear viscosity (η) is defined in Equation 2.5 and it is a quantitative measurement of the internal fluid friction, meaning how much kinetic energy is lost in the system as the momentum from the external force moves though the system [34].

$$\sigma = \frac{F}{A} \tag{2.2}$$

$$\gamma = \frac{h}{x} \tag{2.3}$$

$$\dot{\gamma} = \frac{d\gamma}{dt} \tag{2.4}$$

$$\eta = \frac{\sigma}{\dot{\gamma}} \tag{2.5}$$

In practice, A is the surface area of the geometry used, h is the measurement gap height and F is translated from the torque requested by the rheometer's motor. The shear rate is determined from the plate or cone radius (r) and the angular velocity (ω), seen in Equation 2.6. C/P geometries are often preferred since the shear rate is constant across the sample. For low-viscosity samples or at very low shear rates, C/B geometries are more advantageous since they have a larger surface area which increases the resistance and makes it easier to measure the force required by the rheometer.

$$\dot{\gamma} = \frac{r * \omega}{h} \tag{2.6}$$

Catalytic inks often display a non-Newtonian shear thinning behavior, which means that the viscosity of the ink decreases with increased shear as can be seen in Figure 2.5 compared with a Newtonian sample [17]. At very low shear rates, the viscosity plateaus to a value called the zero shear viscosity (η_0). Shear thinning occurs due to rearrangements in the micro-structure of the sample as a result of shearing.

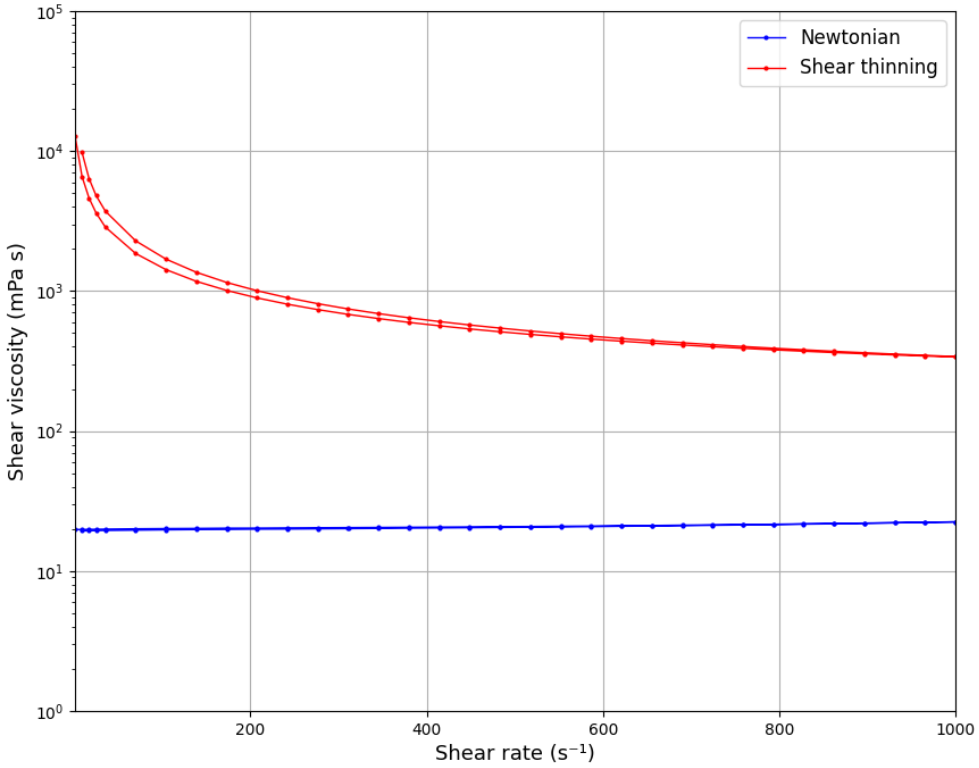

Figure 2.5: Viscosity vs shear rate graph displaying a Newtonian sample (blue) and a shear thinning sample (red). The apparent slight shear thickening seen at high shear rates for the Newtonian sample is a measurement artifact often found for low-viscosity samples and it is due to turbulent flows.

The viscosity of the ink is important for the processing of the ink and the production of electrodes. If the viscosity is too low, the ink would flow freely and spread out too thin and if it is too high, the ink is difficult to work with, there might be issues with distribution and the electrodes could end up very uneven [14]. The ink should ideally have a low viscosity during coating and high viscosity at lower shears to prevent secondary flow [17].

2.5.2 Oscillating measurements

Oscillating measurements can be used to investigate the viscoelastic behavior of a sample. When a fully elastic material is deformed, there is an elastic force that aims to return the sample to its original minimum energy state, like how a stretched-out spring will try to contract back to its original length. In a fully viscous material, the material deforms at a constant rate until the applied stress is removed. The energy is dissipated and the deformation is permanent. Many materials including catalytic ink and ionomer dispersions fall somewhere in between and are therefore called viscoelastic. Small amplitude oscillatory shear is the most common method to measure viscoelastic properties with a rotational rheometer. The sample is oscillated about its equilibrium position in a continuous cycle between the geometries. The upper plate or cone oscillates at a given stress or strain amplitude and frequency. Controlled strain measurements are used in this thesis which means that the angular displacement is controlled and the torque required for it is measured which allows the shear stress to be calculated. The ratio of applied strain to measured stress gives the complex modulus (G^*) as seen in Equation 2.7. It is a quantitative measure of the material's resistance to deform.

$$G^* = \frac{\sigma_{max}}{\gamma_{max}} \tag{2.7}$$

For a fully elastic material, the stress is proportional to the strain meaning that the maximum stress occurs at the maximum strain. For a fully viscous material, the stress is instead proportional to the strain rate meaning the greatest stress is found where the flow rate is the highest. The stress and strain are therefore out of phase by 90°. A material with a phase angle (δ) of 0° is purely elastic and 90° is purely viscous. Viscoelastic materials land somewhere in between. The elastic modulus (G') and viscous modulus (G") can be calculated from the complex modulus and phase angle using Equations 2.8 and 2.9.

$$G' = G^* \cos\delta \tag{2.8}$$

$$G'' = G^* \sin\delta \tag{2.9}$$

The elastic modulus, sometimes referred to as the storage modulus, represents the storage of energy. The viscous modulus, also called the loss modulus, represents the loss or dissipation of energy. They are orthogonal to each other and the complex modulus is therefore often represented as a complex number as in Equation 2.10 where G' is the real part and G" is the imaginary part of G^*.

$$G^* = G' + iG'' \tag{2.10}$$

Catalytic inks are viscoelastic and generally have a linear viscoelastic region where G' is parallel with G" and the elastic modulus is higher than the viscous modulus. After a certain strain where the phase angle is 90°, the ink is no longer able to elastically buffer, and G" drops rapidly to 0. An example of this can be seen in Figure 2.6.

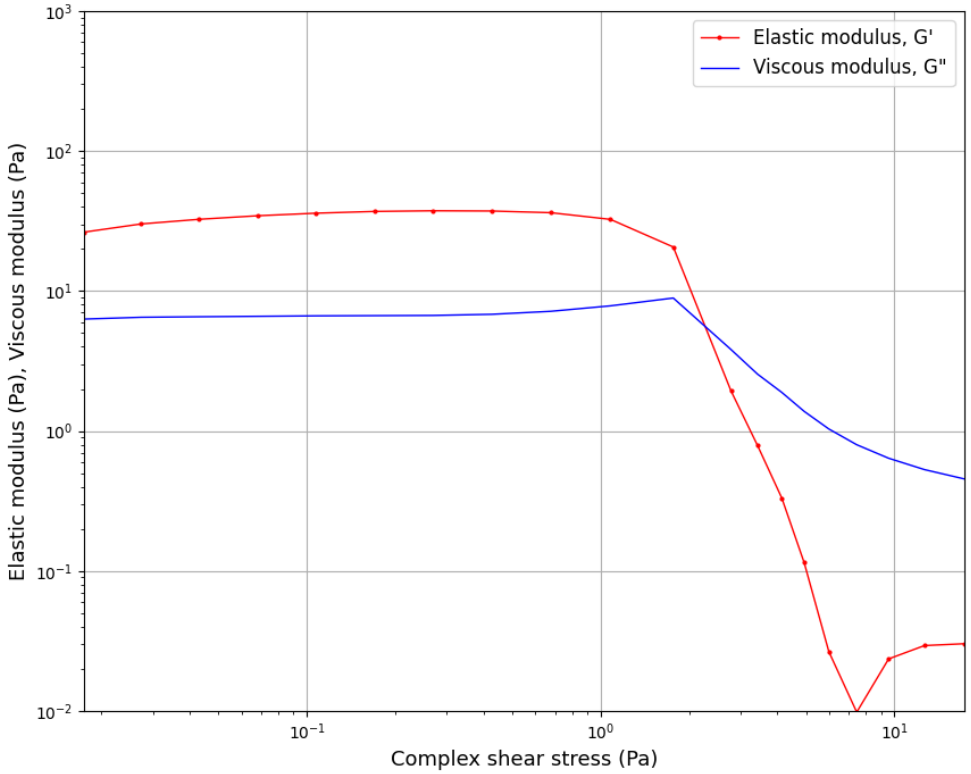

Figure 2.6: Elastic modulus and viscous modulus vs shear stress for a viscoelastic catalytic ink. G" is the viscous modulus (blue) and G' is the elastic modulus (red).

Due to the electrode production methods used at PowerCell, a desirable viscoelastic behavior is high modulus with G' being around 10 X higher than G" as well as elastic buffering up to around 1 Pa.

2.6 Polarization under different operation conditions

To characterize the properties of the finished MEA, several different single-cell sub-scale tests can be performed. The one used in this work is polarization at normal operating conditions. Single-cell sub-scale testing involves a single small MEA being mounted in an FC testing station.

Two important parameters of the operating conditions are the relative humidity of the reaction gas (RH) and coolant inlet temperature T_c. Lower temperatures decrease the catalytic activity and decrease the mass transport of water which combined with high RH leads to an increased risk of flooding the pores. Lower relative humidity and higher temperature often lead to lower proton conductivity as the membrane and ionomer binder in the CL dries out.

The polarization curve is the voltage over current density and it generally decreases with increasing current density. The voltage at 0 A/cm^2 is called the open circuit potential and it has a theoretical value of 1.23 V but is in reality a bit lower due to hydrogen crossover. The rest of the curve can be divided into three regions depending on what type of voltage loss is the most dominant. The first is the kinetic region seen at around 0.1 A/cm^2. The dominant losses in this region are activation losses and are mostly dependent on the ORR kinetics [3]. The second region is the Ohmic region. Here the Ohmic losses are the most prominent. They depend mostly on the conduction resistances in the MEA for both electrons and protons and can be described according to Ohm's law seen in Equation 2.11. This region is linearly decreasing with increasing current density and the resistance is proportional to the slope.

$$U = I \cdot R \tag{2.11}$$

The final region found at high current densities is the mass transport region and can often be seen as a change in the slope after the Ohmic region. In the mass transport region, the CL pores tend to flood with water that can not be transported away as quickly as it is being produced. An example of a polarization curve can be seen in Figure 2.7. The first sharp decrease is the activation losses. The Ohmic region is found between $\sim$ 0.2 – 1.9 A/cm^2 and after that, mass transport is the dominant reason behind voltage loss.

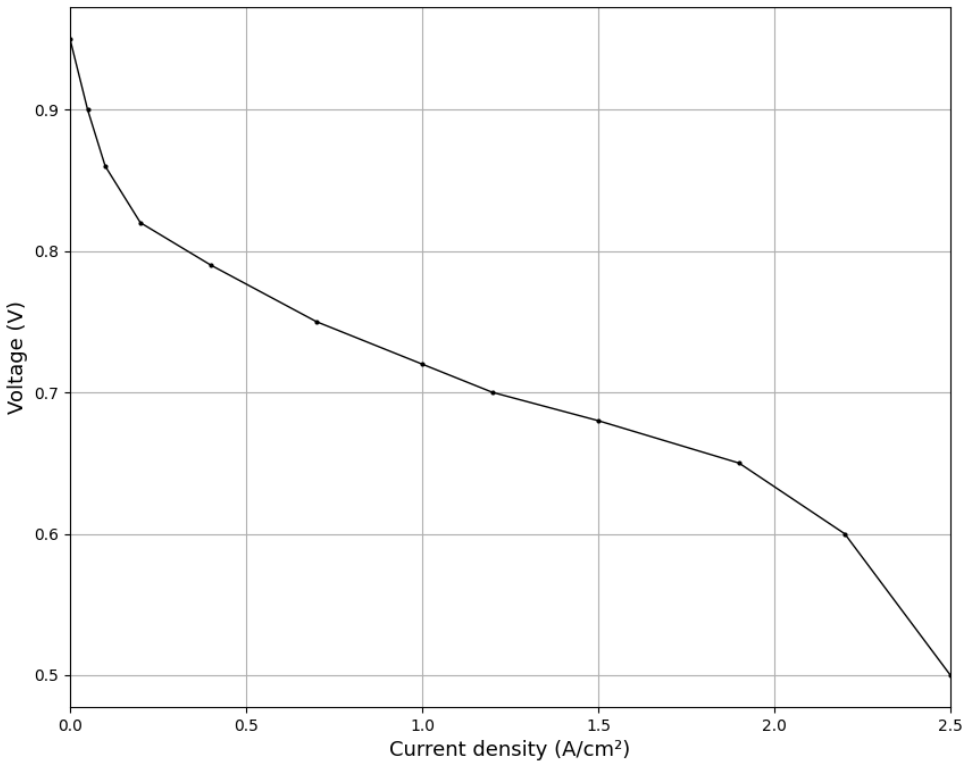

Figure 2.7: Typical polarization curve showing cell voltage over current density.

3
Methods

3.1 Materials

The ionomers tested come from suppliers A, B, C, and D, and the specific ionomers tested are found in Table 4.1.

Table 3.1: Ionomers studied in dispersions and inks.

Name	Type	EW [g/mol]	IEC [meq/g]	Side chain length
A1	PFSA	790	1.23 – 1.30	Short
A2	PFSA	830	1.17 – 1.23	Short
B1	PFSA	1000	1.03 – 1.12	Long
C1	PFSA	800	1.25	Medium
D1	sPPX-H+	-	2.8 – 3.1	-

The solvents used are water (H_2O), ethanol (EtOH), 1-propanol (NPA), 2-propanol (IPA), and tert-butanol (TB). The same 50% platinum nanoparticles on carbon black catalyst will be used in all ink samples. The support is an HSAC which makes it appropriate for cathodes.

Inks are coated on glass fiber-reinforced PTFE films. Subscale MEAs are made out of cathodes prepared using the material listed above, a standard anode composed of ionomer B1 and PFSA membranes.

3.2 Sample preparation

Ionomer dispersions and inks are prepared in 15 ml LDPE, 30 ml HDPE, 20 ml glass, or 50 ml glass bottles. Plastic bottles are always used for the roller-shaker while glass is used for the ultrasonic disperser as they have wider necks.

3.2.1 Ionomer dispersions

The ionomer is weighted and diluted with solvent and water to reach the appropriate concentration for the dispersions. For most samples, either 10 g or 20 g of dispersion is mixed. Ionomers A1, A2, and B1 are purchased in premixed dispersions with 20 – 25 wt% ionomers in a solvent, and the ionomers C1 and D1 were purchased as solids. C1 is dissolved into a 25 wt% dispersion with a 60:40 (w/w) NPA/H_2O solvent

matrix which is rolled for 24 h at 50 rpm as recommended by the supplier. The progression of the dissolution can be seen in Figure 3.1. D1 is dissolved according to supplier recommendation into a 5 wt% solution in a 50:50 (w/w) alcohol/H_2O solvent matrix which is stirred with a magnetic stir bar on a 60 °C hot plate for 24 – 48 h. The alcohols used are NPA and IPA. The progression of the dissolution can be seen in Figure 3.2.

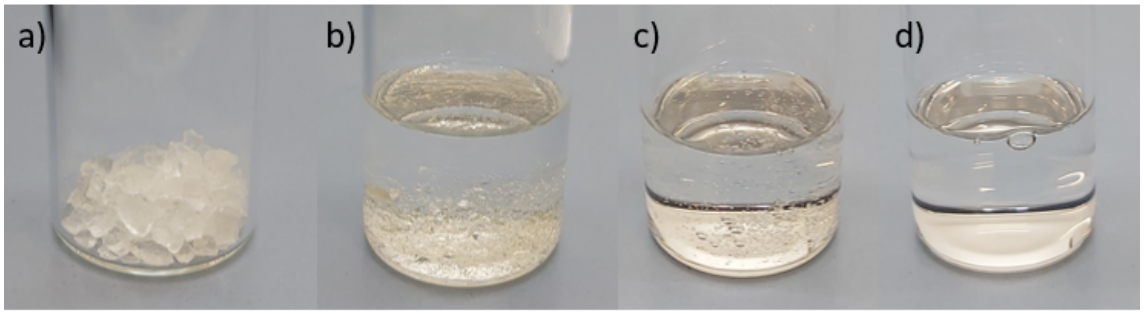

Figure 3.1: Dissolution of C1 ionomer into a 25 wt% dispersion with a 60:40 (w/w) NPA/H_2O solvent matrix. a) shows pure ionomer chunks, b) shows ionomer after solvents have been added, c) shows the system after 4 h on a roller shaker at 50 rpm where some ionomer gel can still be found at the bottom and d) shows the system after 24 h on a roller shaker at 50 rpm where the ionomer dispersion is fully homogeneous.

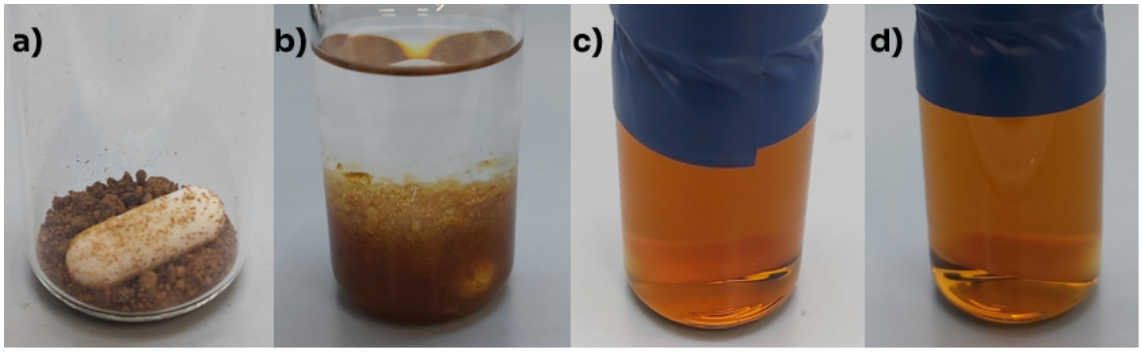

Figure 3.2: Dissolution of D1 ionomer into a 5 wt% solution with a 50:50 (w/w) IPA/H_2O solvent matrix. a) shows pure ionomer chunks with a stir bar, b) shows ionomer after solvents have been added, c) shows the system after 2 h on a heated stir plate at 60 °C where some ionomer is still undissolved d) shows the system after 24 h on a heated stir plate at 60 °C where the ionomer dispersion is fully homogeneous.

3.2.2 Catalytic ink

Untreated inks are mixed by first wetting the catalyst powder with water to avoid spontaneous combustion. The ionomer and organic solvent are added when the catalyst is fully wet. ZrO_2 beads or magnetic stir bar is added and the inks are then left to mature overnight on a stir plate or the roller shaker before dispersion

and heat treatment. Inks made with pre-heated ionomer dispersions are made by first mixing and heating ionomer dispersions according to Sections 3.2.1 and 3.2.3. Catalyst powder is added to a new bottle with either a stir bar or ZrO_2 beads and the appropriate amount of ionomer/solvent dispersion is added. The ink is then left to mix overnight before further dispersion.

3.2.3 Heat treatment

Samples are heat treated by suspending the bottles in a stirring water bath as seen in Figure 3.3 for the allotted time. They are cooled down by running cold water over the bottle after the heat treatment is finished.

Figure 3.3: Heat treatment set up consisting of a beaker of water with a magnetic stirrer on a hot plate fitted with a temperature probe. The sample is clamped and held suspended in the water.

3.2.4 Dispersion

Due to the catalyst particles' tendency to clump together and agglomerate, additional dispersion of the ink is necessary after mixing. This is done either with a roller shaker (RS) or with an ultrasonicator (US). Previous experiments at PowerCell have found that different dispersing methods work best for different catalysts and the one used for the inks in this thesis work tends to disperse better with ultrasonic dispersion as the roller shaker does not input enough energy to break up the catalyst agglomerations. Ultrasonic dispersion uses a Digital Ultrasonic Device UP400St from Hielscher Ultrasonics seen in Figure 3.4. 20 kWs of energy is added with a 14 mm sonotrode at 30% amplitude. During the US dispersion, the ink is stirred with a magnetic stirrer to ensure even sonication, and the ink bottle is immersed in a cool water bath to avoid overheating. The roller shaker is a Phoenix Instrument RS-TR10 seen in Figure 3.5 using 2 mm ZrO_2 beads which mix and disperses the ink at the same time. 3 times the mass of the final ink is added in 2

mm ZrO_2 beads to the ink bottle. The bottle is then left on the RS at 50 rpm for the determined dispersion time.

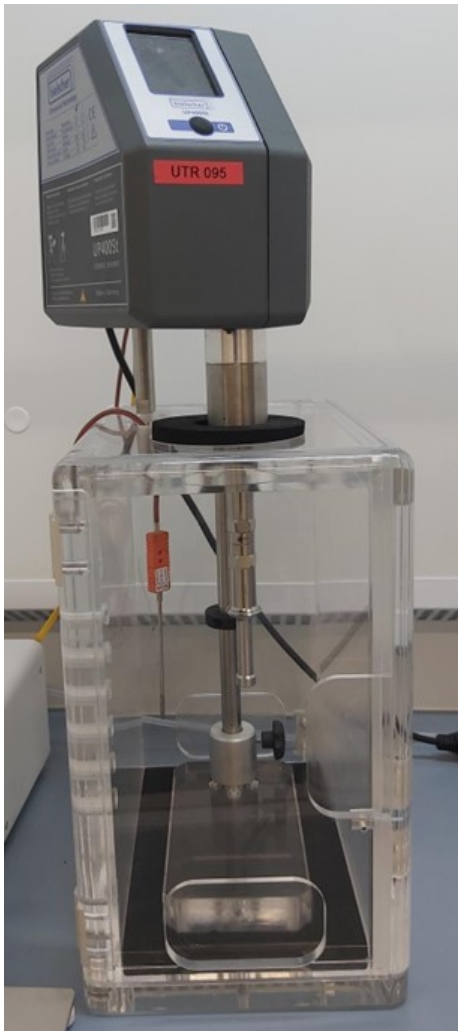

Figure 3.4: Hielscher Ultrasonics Digital Ultrasonic Device UP400St fitted with 14 mm sonotrode.

Figure 3.5: Phoenix Instrument RS-TR10 roller shaker used for mixing and dispersing catalytic ink.

3.3 Rheological measurements

Rheological measurements are conducted at 25 °C on a Kinexus rotational rheometer from Netzsch using 4° angle smooth stainless steel cone with 40 mm diameter (C/P 4/40) as seen in Figure 3.6 for all ionomer dispersions and inks. For very low viscosity samples, a 25 mm diameter stainless steel double gap C/B geometry is used. Measurements are controlled using the rSpace software for rotational rheometers by Netzsch.The standard rheological procedure run on most samples first runs a rotating measurement which ramps the shear rate from 1 to 1000 s^{-1} and measures the shear viscosity of 30 points. 6 points are taken at 1000 s^{-1} before the procedure ramps back down to 1 s^{-1} again. An oscillating measurement follows which keeps a constant frequency of 1 s^{-1} and increases shear stress logarithmically from 0.01 to 100 Pa, taking 5 samples per decade. This procedure is then repeated for three total runs. All graphs display the final run.

Figure 3.6: Kinexus rotational rheometer fitted with C/P 4/40 with a solvent trap in loading position (left) and close up of set up in loaded position with catalytic ink sample (right). During measuring, the geometry and sample are covered with a hood to minimize evaporation and protect from splashing.

3.4 Decal and MEA preparation

MEAs are produced using a decal transfer procedure. First, both anode and cathode decals are made and using the Electrode decal preparation procedure described below. MEAs are then assembled according to the MEA preparation procedure.

3.4.1 Electrode decal preparation

The decals are first made by pipetting a few ml of ink on a glass fiber-reinforced PTFE carrier material attached to an MTV CX4 Film applicator. The ink is spread with a speed of 40 mm/s by a doctor blade with a gap height of 100 μm as seen in Figure 3.7. The decal is then allowed to dry under a plexiglass cover in a climate-controlled room at 23 °C as seen in Figure 3.8.

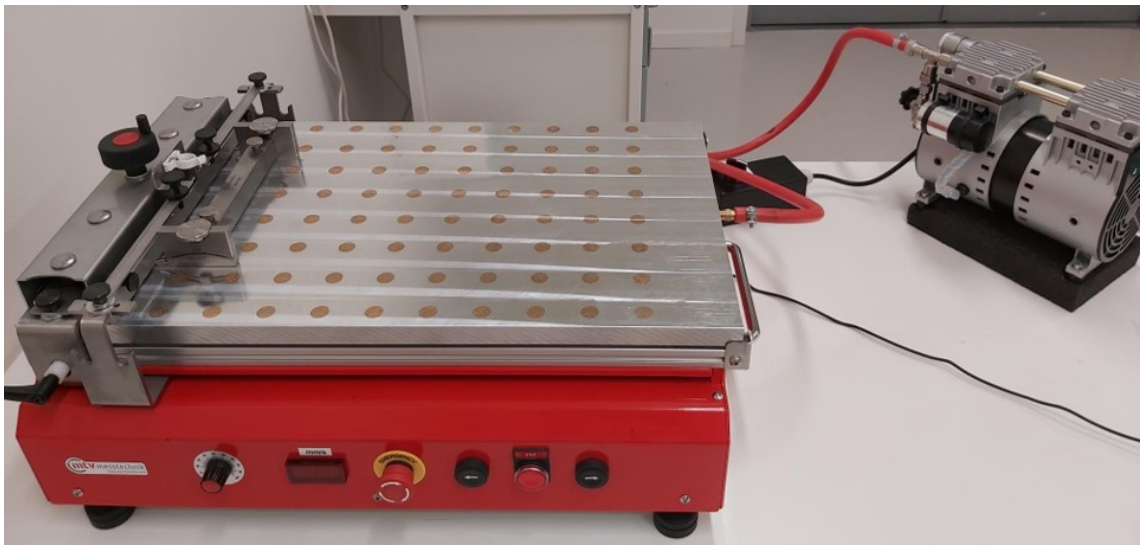

Figure 3.7: MTV CX4 Film applicator with doctor blade used for electrode coatings.

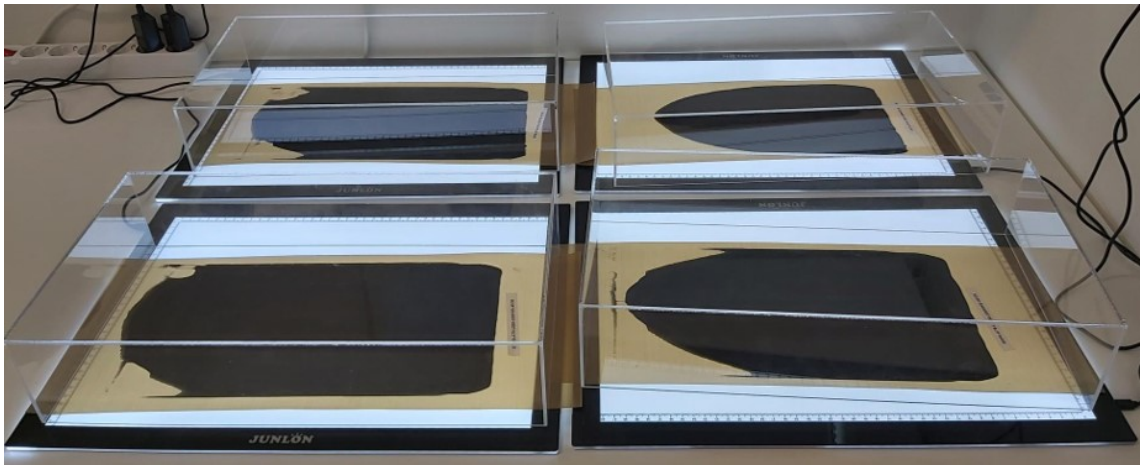

Figure 3.8: Drying setup for coated electrode decals consisting of a light table and a plexiglass hood in a climate-controlled room at 23 °C.

3.4.2 MEA preparation

MEAs are prepared by cutting an anode electrode, a membrane, and an anode electrode to size and hot pressing together to form the CCM. The GDLs and subgaskets that allow mounting in the test station are added with a hand-held heating tool. The final MEA has an active area of 25 cm^2.

3.5 Sub-scale testing

Single-cell sub-scale testing is done according to PowerCells proprietary procedure which begins with conditioning the MEA for 12 h. The voltage is tested at 12

points at current densities between 0.0 and 2.5 A/cm^2. Polarization is done at normal operating conditions which means that the coolant inlet temperature is 65 °C and the relative humidity of the reaction gas is 60%.

3.6 Microscopy

Microscope pictures are taken with a Leica DVM6 A digital microscope from Leica Microsystems using a FOV 3.60 or a FOV 12.55 zoom objective seen in Figure 3.9.

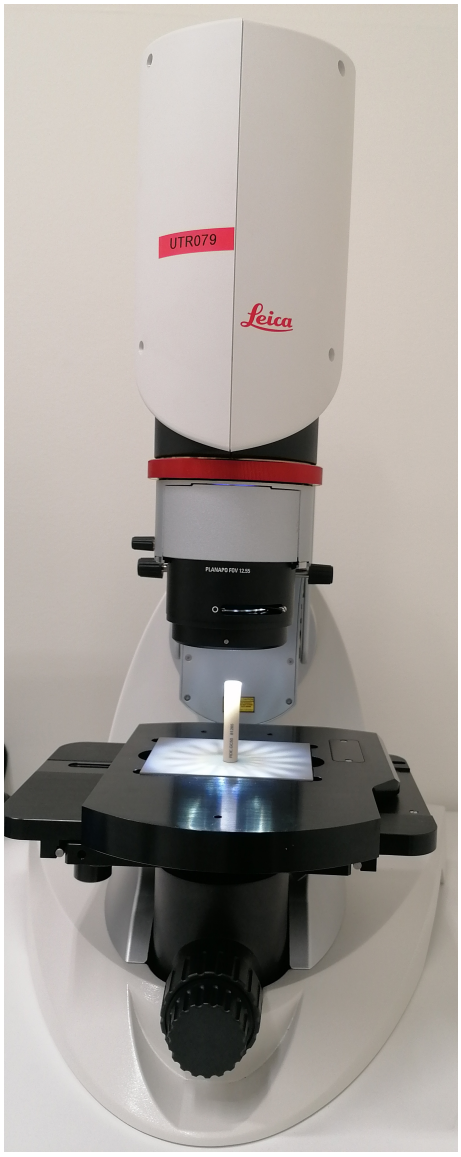

Figure 3.9: Leica DVM6 A digital microscope from Leica Microsystems equipped with a FOV 12.55 zoom objective.

4

Results and Discussion

4.1 Temperature influence on ionomer dispersions using different PFSA ionomers

All of the different PFSA-based ionomers were mixed into dispersions according to Table 4.1.

Table 4.1: Dispersion recipes for investigating differences between ionomers.

Ionomer	Ionomer amount [wt%]	Alcohol	Alcohol amount [wt%]	Water amount [wt%]	Treatment temperature [°C]
A1	5	NPA	80	15	50
A2	5	NPA	80	15	50
B1	5	NPA	80	15	50
C1	5	NPA	80	15	50

The viscosity of these dispersions was tested right after mixing and before any heat treatment (within 15 minutes), after having been heat treated for 1 h at 50 °C, and after being heat treated for 3 h total at 50 °C. Figure 4.1 shows the viscosity at 100 s^{-1} for all ionomer dispersions at all stages of treatment.

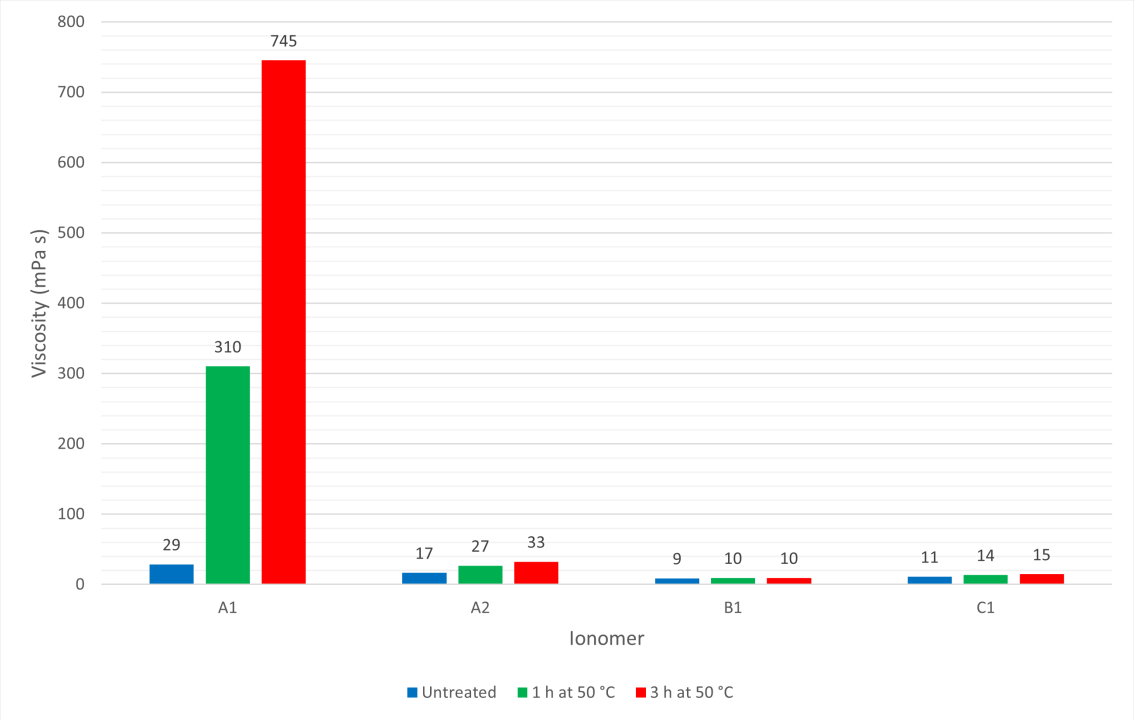

Figure 4.1: Viscosity measurement at 100 s^{-1} for ionomer dispersions mixed according to Table 4.1. The ionomers A1, A2, B1, and C1 were tested before any heat treatment (blue), after being heated in a 50 °C water bath for 1 h (green), and after being heated for 3 h (red).

All 5 wt% ionomer solutions with 80 wt% NPA and 15 wt% H_2O had low viscosity and showed Newtonian behavior before heat treatment. In accordance with supplier documents provided by supplier A, the SSC ionomers, A1 and A2 increased in viscosity as a result of the heat treatment. The effect was significantly more pronounced for ionomer A1 which has a lower EW of 790 g/mol_{SO_3} than A2 which has an EW of 830 g/mol_{SO_3}. Ionomer A1 started to display a shear thinning behavior after being heated which is not observed for any other ionomer.

For LSC ionomer B1, no increased viscosity or shear thinning behavior was observed even after 3 h heat treatment at 50 °C. The same is true for MSC ionomer C1 which only showed a very small increase.

The lower viscosity and effect of heating on the A2 ionomer compared to A1 shows that the EW is strongly responsible for the morphology of the ionomer dispersion as argued by Loppinet et al. [25]. However, seeing as the EW of MSC ionomer C1 is very similar to A1 and has a value between A1 and A2 but thickened less than either, it is clear that the side chain chemistry is also relevant. A shorter side chain as well as lower EW makes the ionomer more prone to thickening.

4.2 PFSA ionomer dispersions with varying solvent matrix

The solvent matrix affects the morphology of the ionomer which can be seen as viscosity differences in the dispersions. Varying solvent matrices were tested for ionomer A1 as it has the strongest thickening behavior and B1 since it can be considered a standard LSC ionomer.

4.2.1 Temperature and solvent influence on A1 ionomer

In order to investigate how dependent the ionomer A1 is on the alcohol concentration, dispersions were made according to Table 4.2. Figure 4.2 shows the viscosity change over shear rate for all of the different 5 wt% A1 in NPA dispersions.

Table 4.2: A1 dispersion recipes for investigating differences between NPA concentrations.

Ionomer	**Ionomer amount [wt%]**	**Alcohol**	**Alcohol amount [wt%]**	**Water amount [wt%]**	**Treatment temp [°C]**
A1	5	NPA	80	15	50
A1	5	NPA	80	15	80
A1	5	NPA	57.5	37.5	50
A1	5	NPA	57.5	37.5	80
A1	5	NPA	37.5	57.5	80

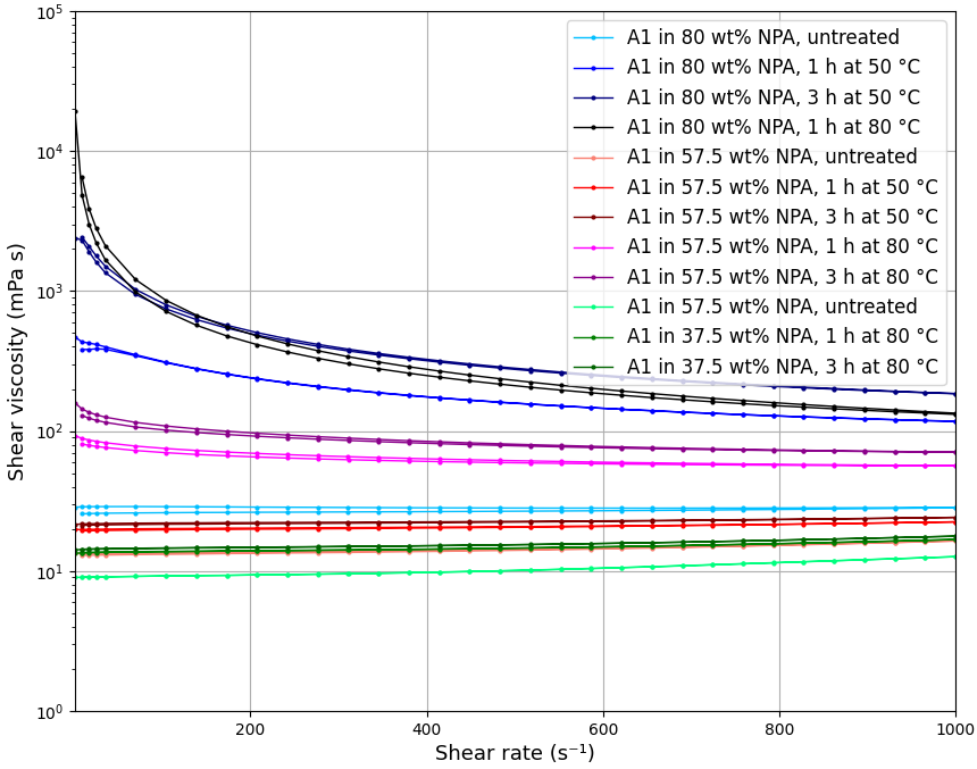

Figure 4.2: Viscosity vs shear rate measurement for ionomer dispersions mixed according to Table 4.2 tested before any heat treatment, after being heated in a water bath for 1 h and after being heated for 3 h. The dispersions are 80 wt% NPA and 15 wt% H_2O heated at 50 °C (blue), 80 wt% NPA and 15 wt% H_2O heated at 80 °C (black), 57.5 wt% NPA and 37.5 wt% H_2O heated at 50 °C (red), 57.5 wt% NPA and 37.5 wt% H_2O heated at 80 °C (magenta) and 37.5 wt% NPA and 57.5 wt% H_2O heated at 80 °C (green).

Lower alcohol concentrations lead to less viscous dispersions and a smaller viscosity change as a result of heating. This indicates that the alcohol interaction with the backbone is what leads to the ionomer stretching out. By increasing the temperature, even lower alcohol content dispersions can thicken up. When the alcohol content is low, the hydrophobicity of the backbone prevents the unfurling of ionomer micelles, even when heated at higher temperatures.

Supplier documents from A indicate that different alcohols also affect the thickening behavior. This was investigated for dispersions made from NPA, IPA, and EtOH mixed according to Table 4.3 as well as for NPA, IPA, and TB mixed according to Table 4.4. The viscosity over shear rate can be seen in Figures 4.3 and 4.4 respectively. The viscosity of the dispersions was tested before any heat treatment, after having been heat treated at 50 °C for 1 h, and after being heat treated for 3 h total.

Table 4.3: A1 dispersion recipes for investigating differences between alcohols in the solvent matrix at high alcohol concentrations.

Ionomer	**Ionomer amount [wt%]**	**Alcohol**	**Alcohol amount [wt%]**	**Water amount [wt%]**	**Treatment temp [°C]**
A1	5	NPA	80	15	50
A1	5	IPA	80	15	50
A1	5	EtOH	80	15	50

Table 4.4: A1 dispersion recipes for investigating differences between alcohols in the solvent matrix at lower alcohol concentrations.

Ionomer	**Ionomer amount [wt%]**	**Alcohol**	**Alcohol amount [wt%]**	**Water amount [wt%]**	**Treatment temp [°C]**
A1	5	NPA	57.5	37.5	50
A1	5	IPA	57.5	37.5	50
A1	5	TB	57.5	37.5	50

Due to TB solvent stock already containing 10 wt% water, no dispersion with 80 wt% TB could be prepared. The dispersion with 80 wt% IPA became too thick to test properly and splashed out of the rheometer after 3 h and that measurement is therefore not included. EtOH was not tested with lower alcohol content due to having a very weak response even at high alcohol concentrations.

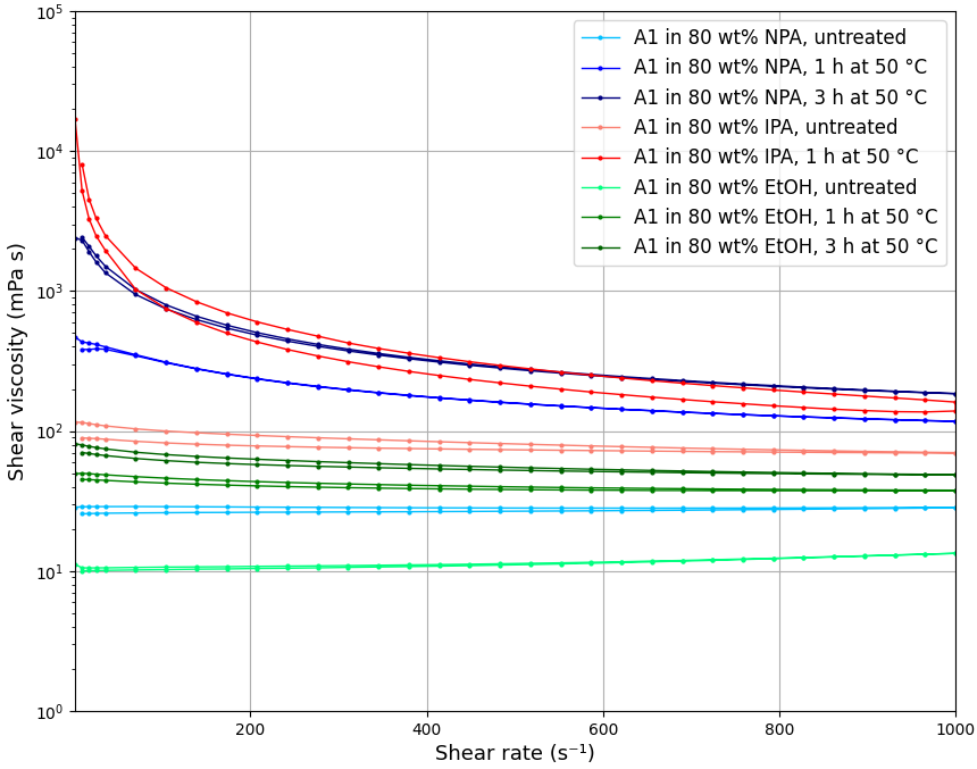

Figure 4.3: Viscosity vs shear rate measurement for ionomer dispersions mixed according to Table 4.3. The alcohols are NPA (blue), IPA (red), and EtOH (green), and the dispersions were tested before any heat treatment, after being heated in a 50 °C water bath for 1 h and after being heated for 3 h.

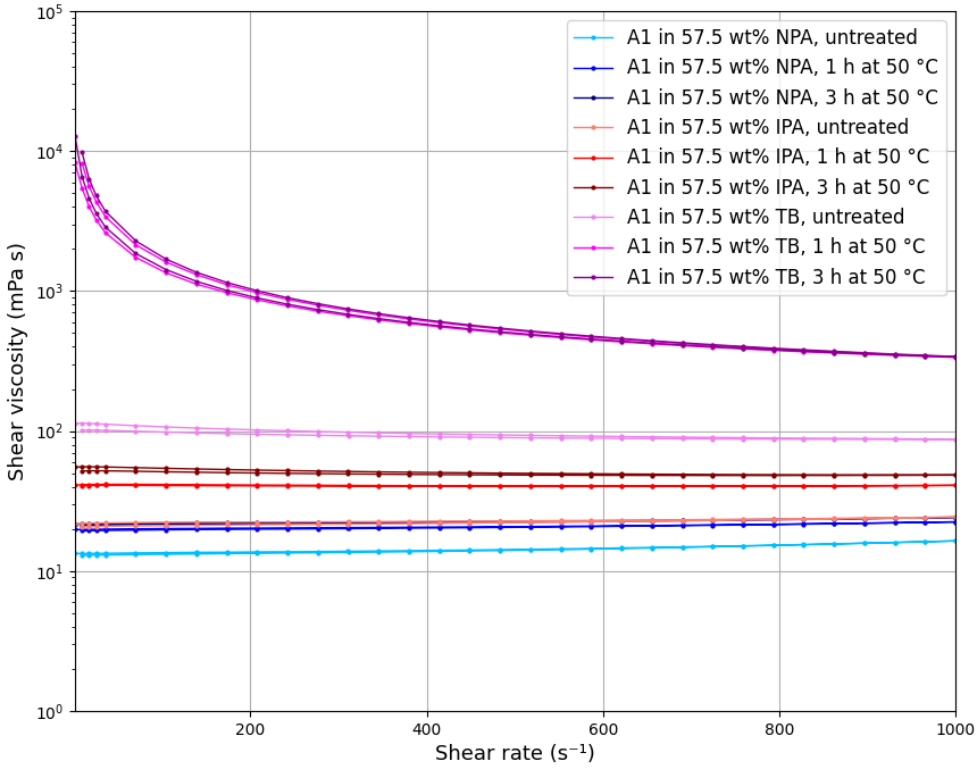

Figure 4.4: Viscosity vs shear rate measurement for ionomer dispersions mixed according to Table 4.4. The alcohols are NPA (blue), IPA (red), and TB (magenta), and the dispersions were tested before any heat treatment, after being heated in a 50 °C water bath for 1 h and after being heated for 3 h.

TB increases the viscosity drastically even before heat treatment and heating at 50 °C for 1 h completely gels it up. The viscosity increased from 85 mPa s for the untreated sample to 1540 mPa s after 1 h of heat treatment at 50 °C at a shear rate of 100 s^{-1}. It also started to display a strong shear-thinning behavior. The same lower alcohol concentration at 50 °C for NPA and IPA only showed a small thickening effect with IPA having a higher viscosity than NPA. The degree of thickening seems to correlate with how large the hydrophobic backbone of the solvent is compared to the functional group as well as how the placement of the functional group in the molecule. The more sterically hindering each solvent is when interacting with the ionomer backbone, the higher the dispersion viscosity. The alcohols can be ordered from the least to the most sterically hindering as: EtOH < NPA < IPA < TB.

To see the effects of mixing different types of alcohols, a dispersion containing a mixture of NPA and TB was mixed and heated for 1 h and 3 h at 50 °C. The result compared to using only NPA or TB as mixed according to Table 4.5 can be seen in Figure 4.5.

Table 4.5: A1 dispersion recipes for investigating viscosity effects of mixed alcohols.

Ionomer	Ionomer amount [wt%]	NPA amount [wt%]	TB amount [wt%]	Water amount [wt%]	Treatment temp [°C]
A1	5	57.5	0	37.5	50
A1	5	28.75	28.75	37.5	50
A1	5	0	57.5	37.5	50

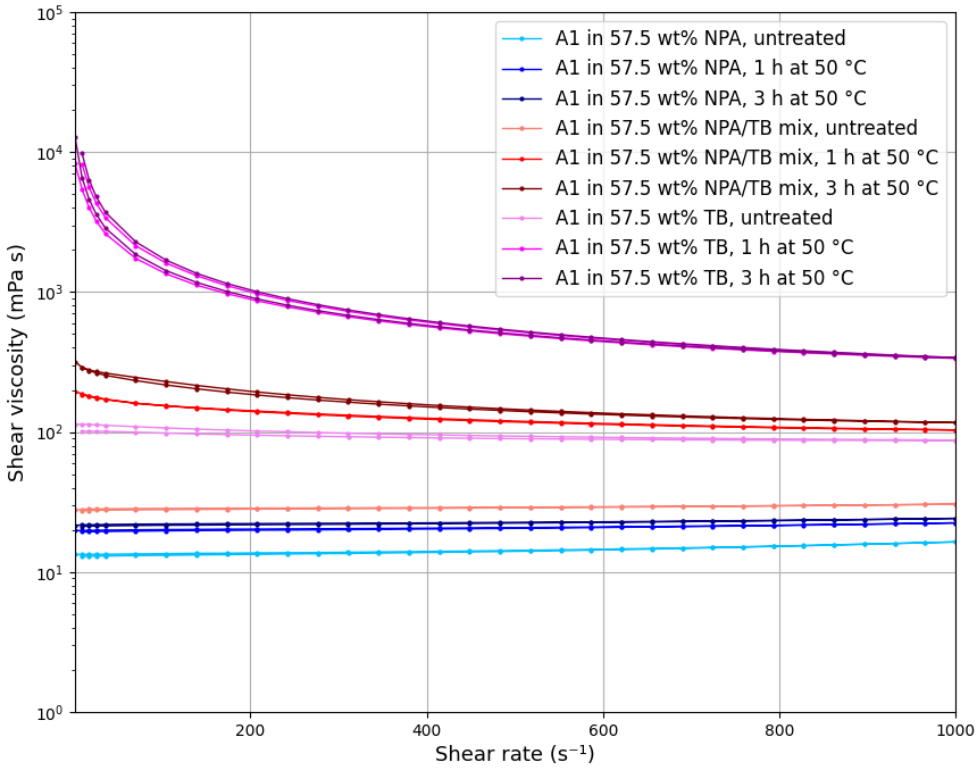

Figure 4.5: Viscosity vs shear rate measurement for ionomer dispersions mixed according to Table 4.5. The alcohols are NPA (blue), 1:1 (w/w) NPA/TB (red), and TB (magenta), and the dispersions were tested before any heat treatment, after being heated in a 50 °C water bath for 1 h and after being heated for 3 h.

When mixing different NPA and TB, the viscosity is somewhere in between the dispersions which only contain one alcohol and the increase appears to scale logarithmically. When the alcohol content is an equal mix of NPA and TB, the viscosity ends up being about one decade above NPA and one decade below TB. This means that several parameters can be altered in order to achieve a desired viscosity when optimizing an ink for processing.

4.2.2 Temperature and solvent influence on B1 ionomer

As can be seen in Subsection 4.2.1, TB clearly has the strongest thickening effect on the SSC ionomer, however Subsection 4.1 shows that LSC ionomer B1 does not thicken even at high alcohol contents in NPA. To see if TB will affect LSC ionomers, a dispersion mixed according to Table 4.6 was prepared. The 11.5 wt% NPA comes from the B1 ionomer stock solution. The total alcohol content is 60 wt% of the solvent matrix.

Table 4.6: B1 dispersion recipe for investigating the effect of heat treatment on a TB based solvent matrix.

Ionomer	Ionomer amount [wt%]	NPA amount [wt%]	TB amount [wt%]	Water amount [wt%]	Treatment temp [°C]
B1	5	11.5	46	37.5	50

As seen in Figure 4.6, there appears to be a very slight increase in viscosity as the dispersion is heated but it is only increased from 21 to 24 mPa s after 3 h of heating at 50 °C, any difference is considered to within the margin of error which according to Netzsch can be as high as 10%, especially for low viscosity samples. No shear thinning was observed.

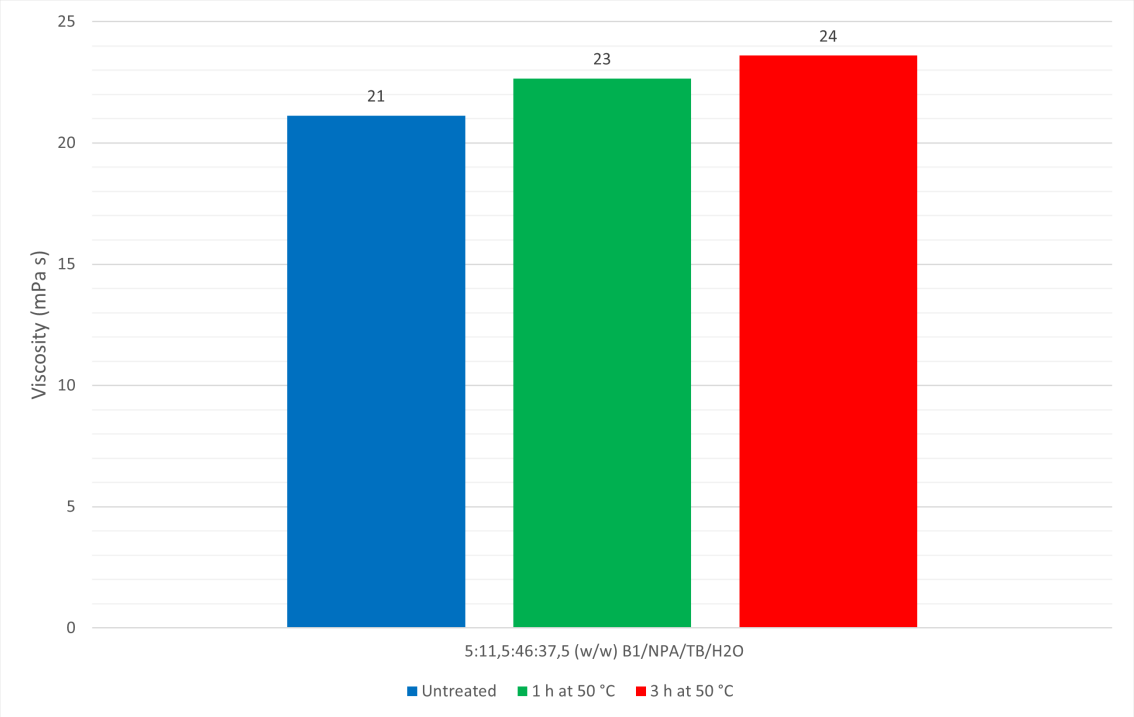

Figure 4.6: Viscosity measurement at 100 s^{-1} for ionomer dispersion mixed according to Table 4.6. The dispersion was tested before any heat treatment (blue), after being heated in a 50 °C water bath for 1 h (green), and after being heated for 3 h (red).

Since the effect of heating is negligible even for high alcohol concentrations and for the most sterically hindering solvent, B1 solutions with lower NPA content, IPA,

and EtOH were not heated. Dispersions were mixed according to Table 4.7 and tested and the viscosity is seen in Figure 4.7.

Table 4.7: B1 dispersion recipes for investigating differences between alcohols in the solvent matrix.

Ionomer	Ionomer amount [wt%]	NPA amount [wt%]	Other Alcohol	Other alcohol amount [wt%]	Water amount [wt%]
B1	5	57.5	-	-	37.5
B1	5	11.5	IPA	46	37.5
B1	5	11.5	EtOH	46	37.5
B1	5	11.5	TB	46	37.5

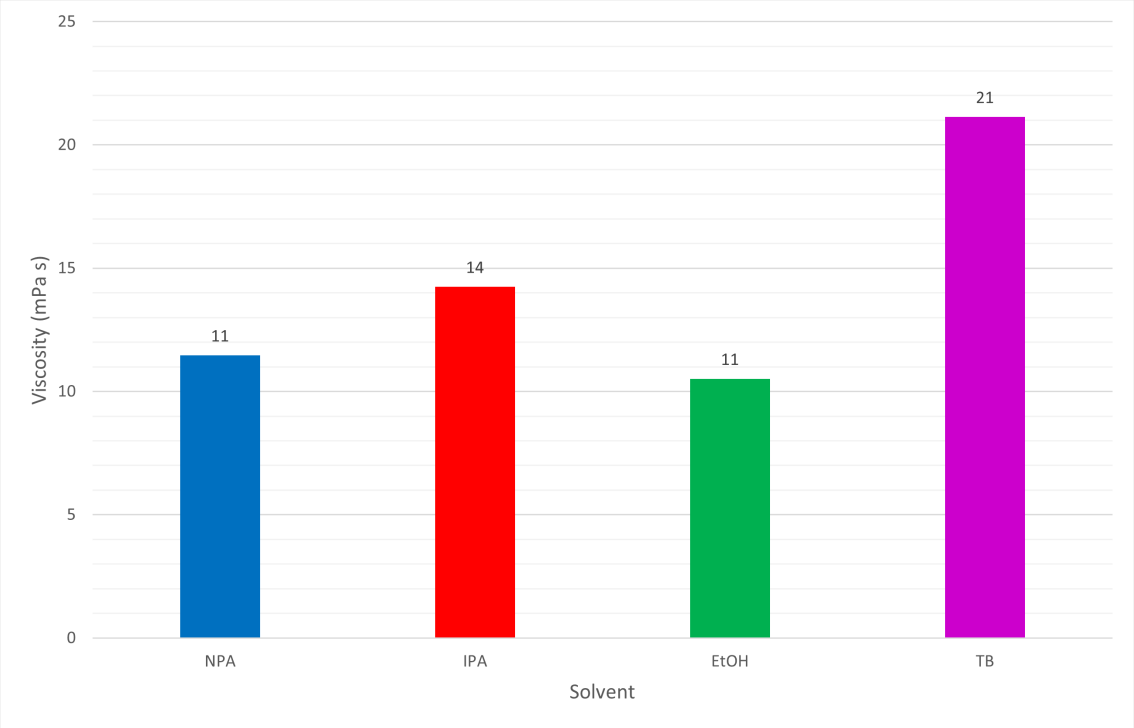

Figure 4.7: Viscosity measurement at 100 s^{-1} for ionomer dispersions mixed according to Table 4.7. The alcohols are NPA (blue), IPA (red), EtOH (green), and TB (purple).

The viscosity of the TB sample is slightly higher than the other solvents. This could indicate that the solvent has some effect on the ionomer. This change is very small when compared to the SSC and low EW A1 ionomer. None of the B1 dispersions showed any shear thinning behavior.

4.3 Temperature influence on ionomer dispersions with varying ionomer content

In order to see the effect ionomer concentration has on the viscosity, dispersions with solvent matrices of 60 wt% NPA and 40 wt% H_2O were mixed according to Table 4.8 and heated for 1 h and 3 h at 50 °C. The results can be found in Figure 4.8.

Table 4.8: A1 dispersion recipes for investigating differences between ionomer concentrations.

Ionomer	Ionomer amount [wt%]	Alcohol	Alcohol amount [wt%]	Water amount [wt%]	Treatment temperature [°C]
A1	5	NPA	57.5	37.5	50
A1	7	NPA	56.5	36.5	50
A1	10	NPA	55	35	50

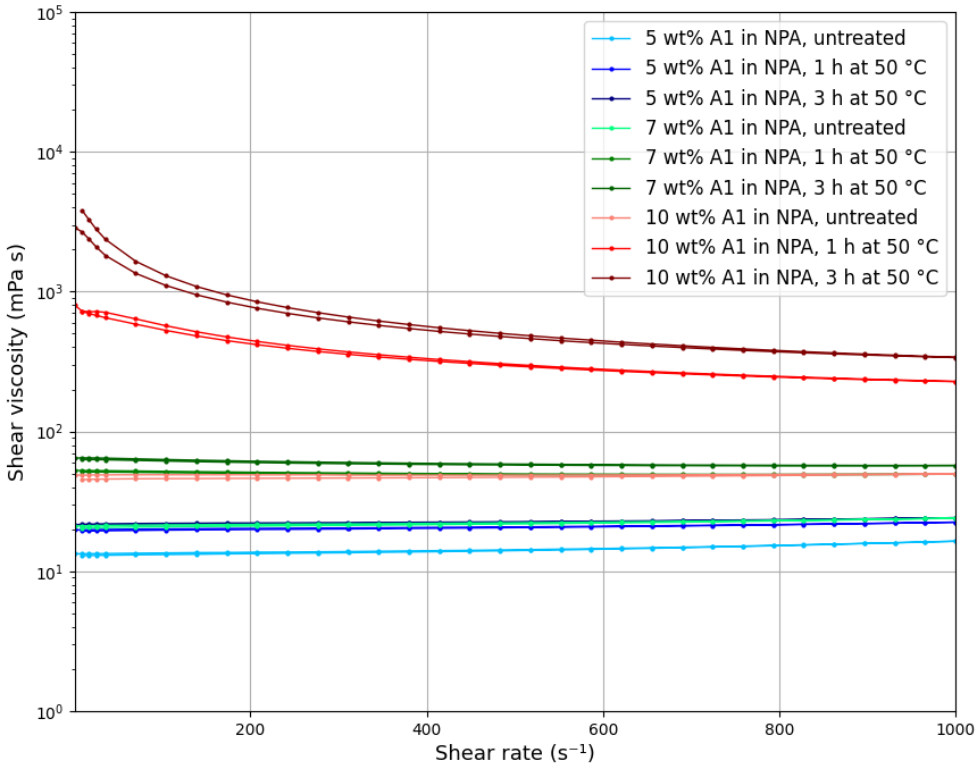

Figure 4.8: Viscosity vs shear rate measurement for ionomer dispersions consisting of A1 ionomer mixed according to Table 4.8. The ionomer concentrations are 5 wt% (blue), 7 wt% (green), and 10 wt% (red). The dispersions were tested before any heat treatment, after being heated in a 50 °C water bath for 1 h, and after being heated for 3 h.

Increasing the ionomer concentration significantly increases the viscosity of the dispersion as well as the effect heating has. This is most likely due to it being easier to form interconnected bundles at higher concentrations.

4.4 Viscosity for HC ionomer in solution

Due to having a very different chemical composition and heating already being a part of the dissolution process proposed by the supplier, the HC ionomer D1 was not heat treated and tested in the same ways as the PFSA ionomers. 5 wt% ionomer was dissolved according to supplier recommendations as described in Section 3.2 using NPA and IPA as seen in Table 4.9. The results are found in Figure 4.9.

Table 4.9: D1 dispersion recipes for investigating differences between alcohols in the solvent matrix.

Ionomer	Ionomer amount [wt%]	Alcohol	Alcohol amount [wt%]	Water amount [wt%]
D1	5	NPA	47.5	47.5
D1	5	IPA	47.5	47.5

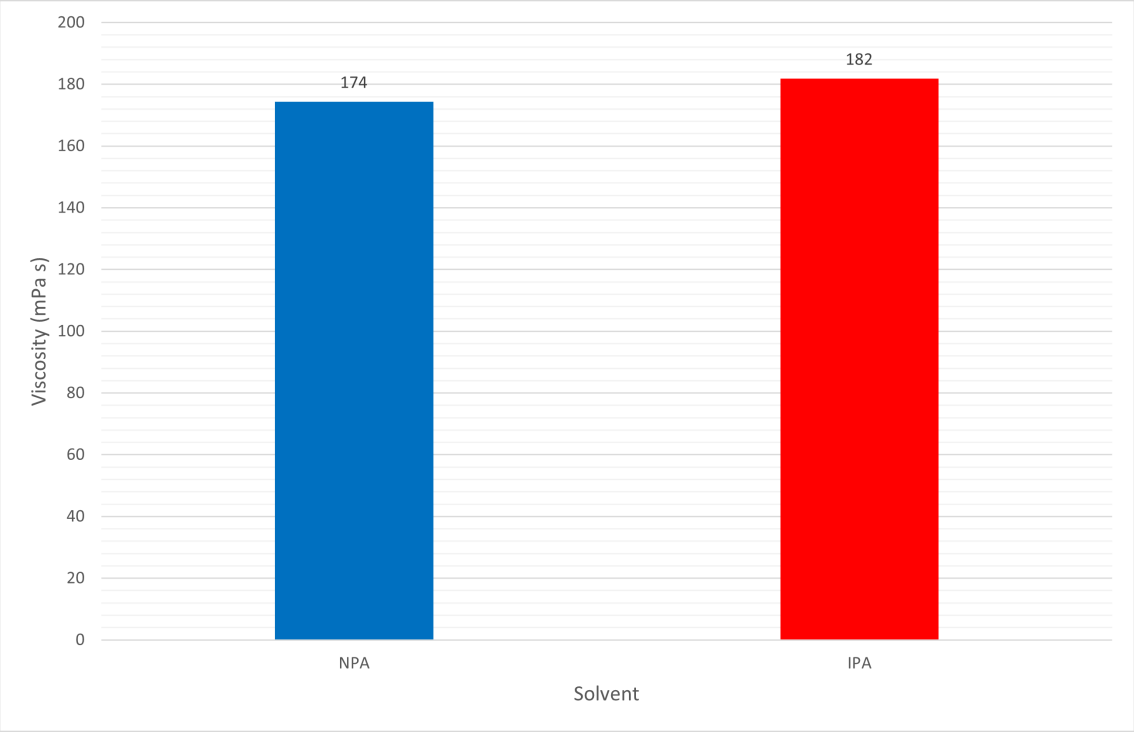

Figure 4.9: Viscosity measurement at 100 s^{-1} for ionomer dispersions mixed according to Table 4.9. The alcohols are NPA (blue) and IPA (red).

Compared with the PFSA ionomers, D1 has a significantly higher viscosity than any of the other untreated ionomers which are all $\leq$ 100 mPa s even at much higher alcohol concentrations and with more sterically hindering solvents. This indicates

that the D1 ionomer has a different structure to the PFSA ionomer in solution and that it most likely does not form the same type of micellar structures that PFSA does. IPA gives slightly higher viscosity than NPA.

4.5 Catalytic inks mixed from ionomer dispersions

The SSC A1 ionomer has varying states in solvents which can be altered in several ways as seen in Sections 4.1, 4.2, and 4.3. The behavior changes further when Pt/C is added and what behavior can be contributed to each component of the catalytic ink is harder to determine than in ionomer dispersions. Several similar inks were made where different ways to alter the ionomer state were implemented. Three different ink component proportions were used in this thesis and they can be seen in Table 4.10.

Table 4.10: Ink recipes used throughout Section 4.5.

Recipe	Ionomer type	Ionomer amount [wt%]	Catalyst amount	Solid content [wt%]	Alcoholic part of solvent matrix [wt%]	Water part of solvent matrix [wt%]
1	PFSA	5	10.3	15.3	60	40
2	PFSA	4.1	8.5	12.6	60	40
3	HC	1.64	8.66	10.3	50	50

4.5.1 High solid content NPA based A1 ink with ultrasonic dispersion

Due to there being a weak thickening effect of ionomer A1 in lower concentrations of NPA, inks based on a 60:40 (w/w) NPA/H_2O solvent matrix are heated at 80 °C. A catalytic ink was mixed according to Table 4.11 which keeps the ionomer concentration to 5 wt%. The ink underwent the same heat treatment as the ionomer dispersions described in Section 4.1.

Table 4.11: Ink recipe and treatment for investigating the effect of heating an ink.

Recipe	Ionomer	Alcohol	Dispersion	Treatment	Treatment temperature [°C]
1	A1	NPA	US 20 kWs	Heating ink after dispersion	80

Figure 4.10 shows a viscosity increase after 1 h of heat treatment compared to the untreated ink but no significant difference between 1 h and 3 h. Figure 4.11 shows a decrease in the elastic modulus after heat treatment.

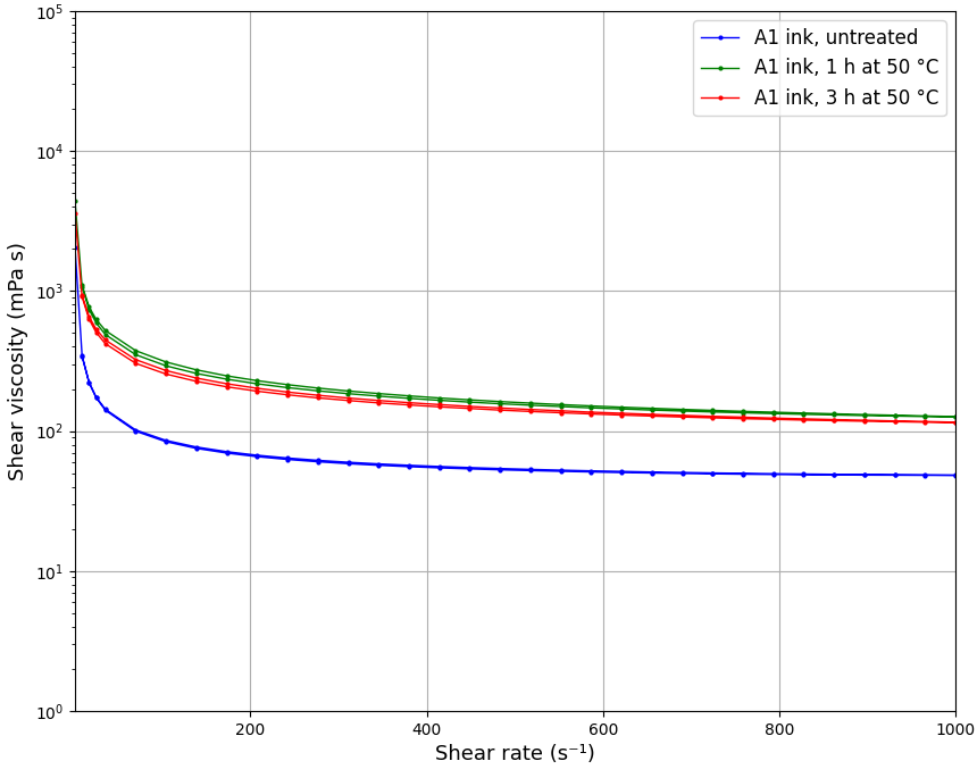

Figure 4.10: Viscosity vs shear rate for ink mixed according to Table 4.11. The ink was tested untreated (blue), after being heated in an 80 °C water bath for 1 h (green) and after being heated for 3 h (red).

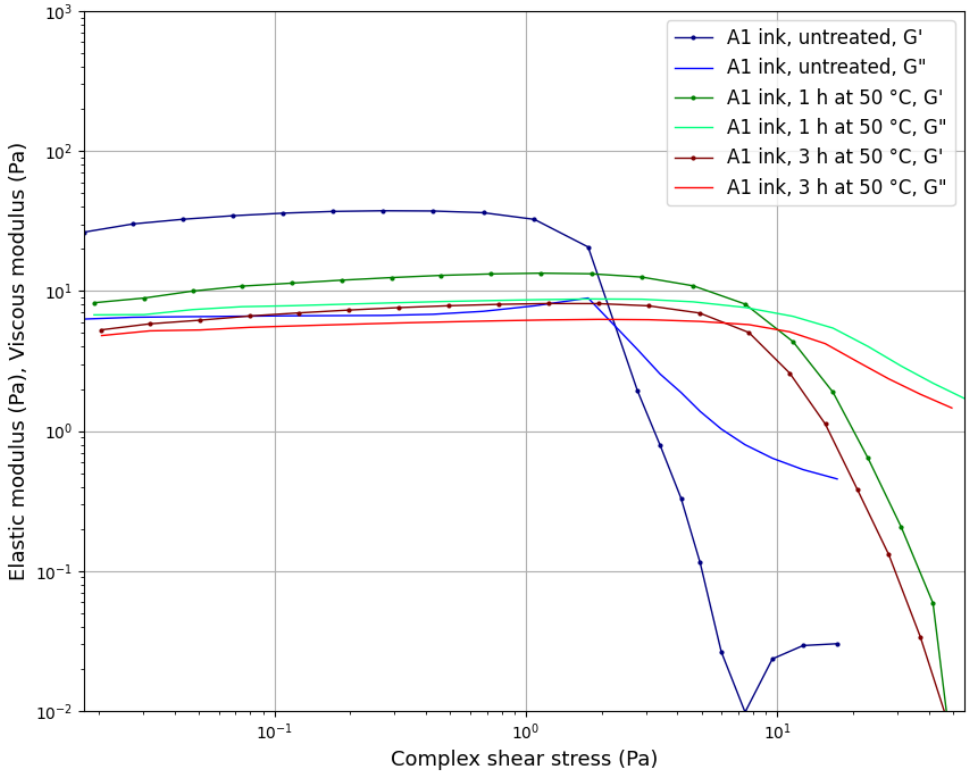

Figure 4.11: Elastic modulus (G') & viscous modulus (G") vs complex shear stress for ink mixed according to Table 4.11. The ink was tested untreated (blue), after being heated in an 80 °C water bath for 1 h (green) and after being heated for 3 h (red).

Decals were prepared from the ink at all stages of treatment Untreated ink gives a fairly homogeneous decal with some cracks while both decals from heated ink are full of holes from bubbles in the ink that popped during drying as can be seen in Figure 4.12 and 4.13.

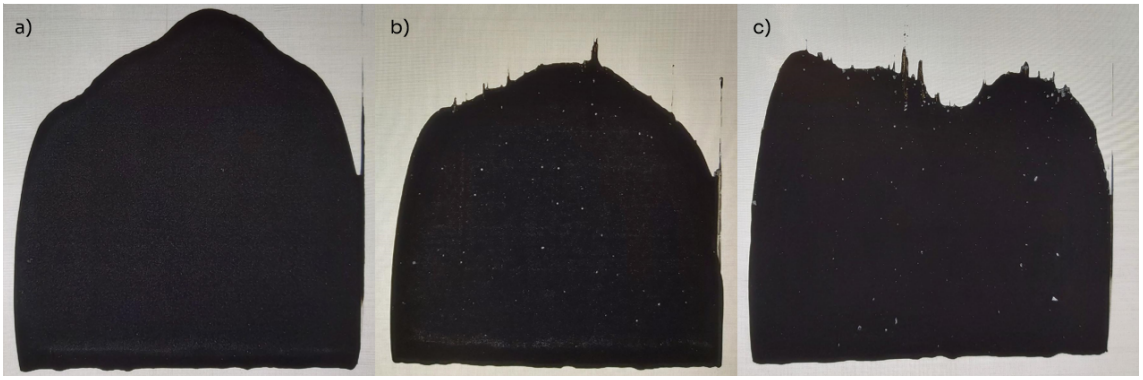

Figure 4.12: Coated decals made from US ink mixed according to Table 4.11 that was heated after mixing. a) is made from untreated ink, b) is made from ink heated in an 80 °C water bath for 1 h, and c) is made from ink heated in an 80 °C water bath for 3 h.

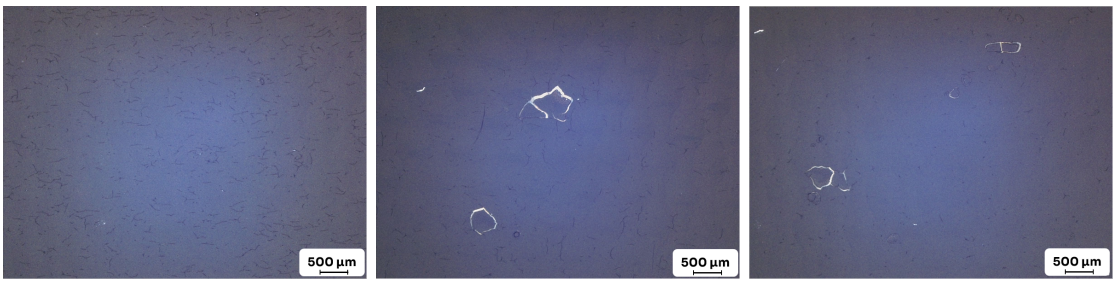

Figure 4.13: Microscope picture of coatings made from ink mixed according to Table 4.11 and dispersed with US. The coatings are made before the ink was heated (left), after being heated for 1 h at 80 °C (middle), and after being heated for 3 h at 80 °C (right).

Similar inks were mixed up according to Table 4.12 using pre-thickened ionomer and solvent dispersions which had been heated for 1 h and 3 h at 80 °C giving the dispersion a viscosity of $\sim$ 170 mPa s and $\sim$ 260 mPa s respectively when sheared at 100 s^{-1}. The rheological behavior of these inks can be seen in Figures 4.14 and 4.15. All three inks were dispersed using the US. Thicker ionomer dispersions prior to mixing result in thicker inks. The modulus is also high for all inks and they increase with thicker starting dispersion.

Table 4.12: Ink recipe and treatments for investigating the effect of pre-treating ionomer before mixing inks.

Recipe	**Ionomer**	**Alcohol**	**Dispersion**	**Treatment**	**Treatment temperature [°C]**
1	A1	NPA	US 20 kWs	Heating ionomer and solvent for 1 h prior to mixing	80
1	A1	NPA	US 20 kWs	Heating ionomer and solvent for 3 h prior to mixing	80

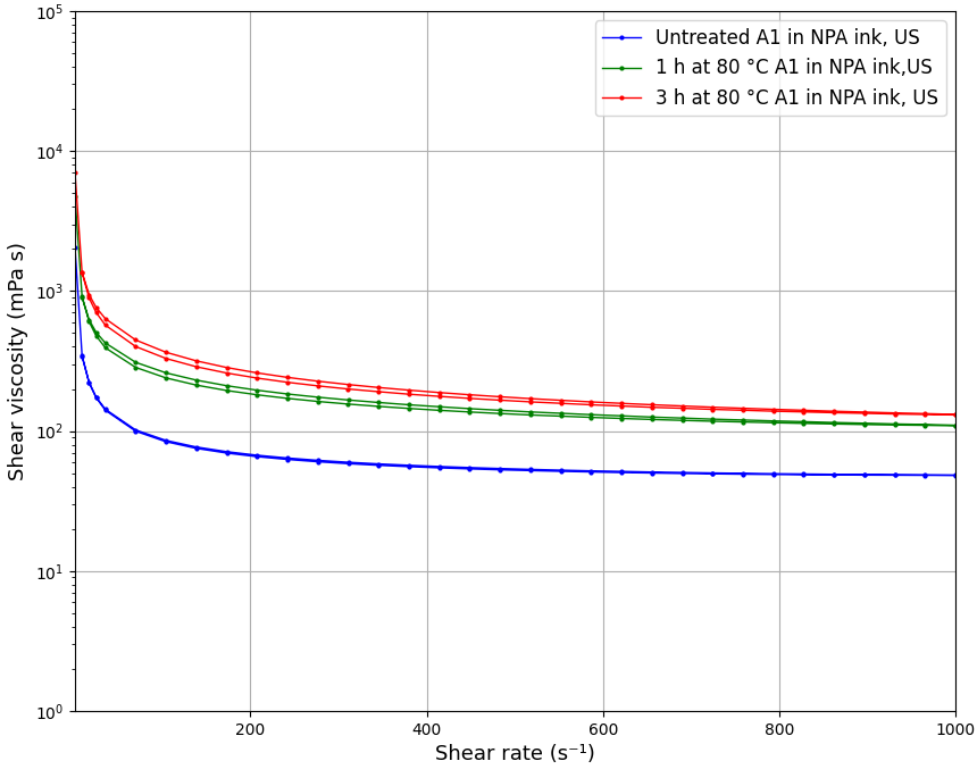

Figure 4.14: Viscosity vs shear rate for ink mixed according to Table 4.12 and dispersed with US. The ink was made from an ionomer dispersion that was untreated (blue), an ionomer dispersion that had been heated in an 80 °C water bath for 1 h (green) and an ionomer dispersion that had been heated for 3 h (red).

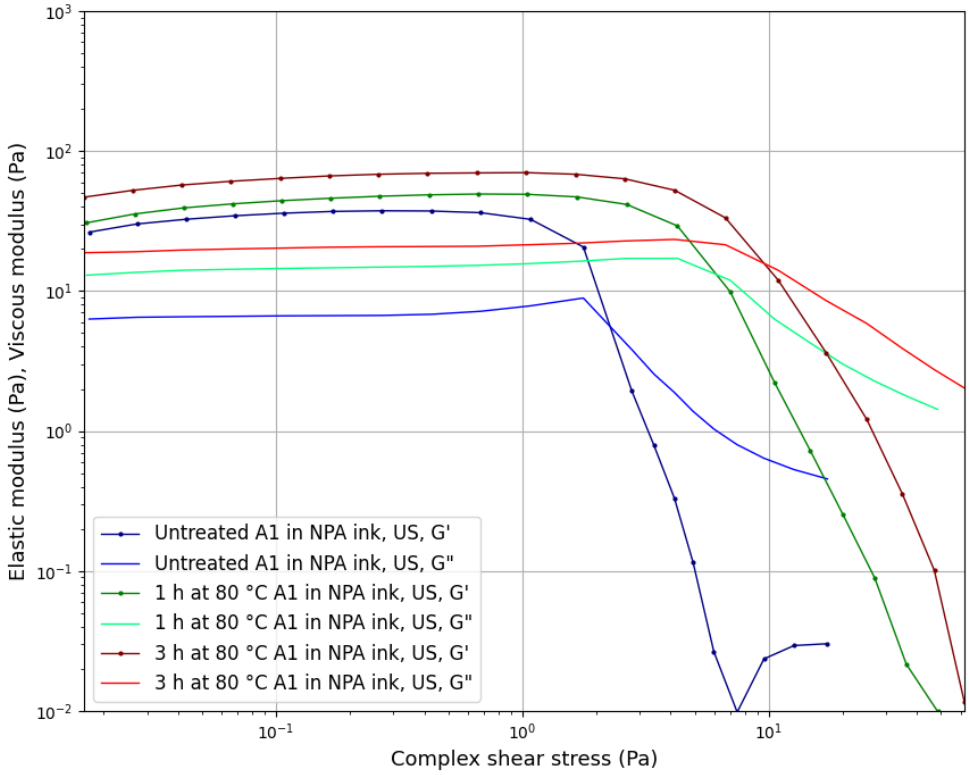

Figure 4.15: Elastic modulus (G') & viscous modulus (G") vs complex shear stress for ink mixed according to Table 4.12 and dispersed with US. The ink was made from an ionomer dispersion that was untreated (blue), an ionomer dispersion that had been heated in an 80 °C water bath for 1 h (green) and an ionomer dispersion that had been heated for 3 h (red).

From the rheological behavior, pre-treating the ionomer dispersion seems advantageous to heating the ink if an increased viscosity is desired. However, both decals made with pre-thickened ionomer dispersions are very poorly dispersed and are covered with large catalyst powder agglomerates as seen in Figure 4.16. The poor dispersion is believed to be due to a combination of the high solid content, poor mixing, and too little dispersion.

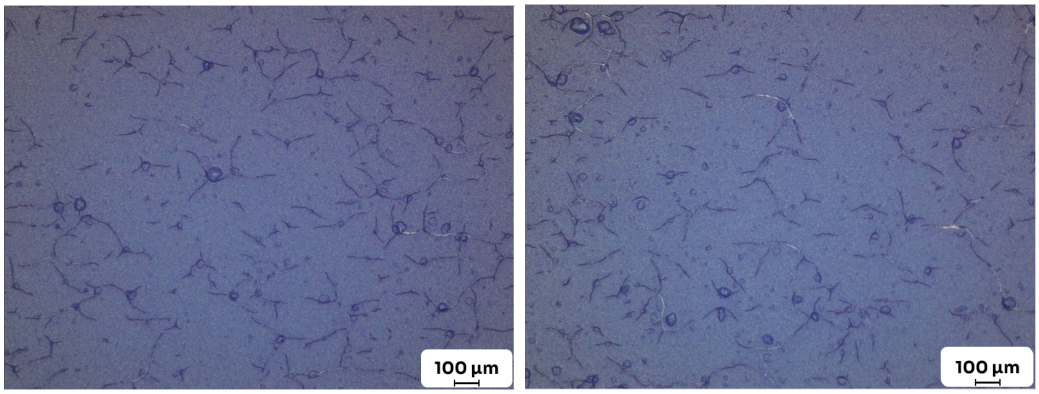

Figure 4.16: Microscope picture of coatings made from ink mixed according to Table 4.12 with ionomer dispersions that had been pre-treated for 1 h at 80 °C (left) and 3 h at 80 °C (right) and dispersed with US. The coating is full of cracks and large catalyst agglomerates.

4.5.2 Lower solid content NPA based A1 ink mixed on roller shaker

Ink with a lower solid content of 12.6 wt% mixed according to recipe 2 in Table 4.10 with NPA as the alcohol and dispersed using the roller shaker were prepared in order to hopefully achieve better mixing. One ink was mixed straight away without any heating, one was made with ionomer that had been heated along with all solvents at 80 °C for 1 h, and one was made with ionomer heated for 3 h as seen in Table 4.13. These ionomer dispersions had a viscosity of $\sim$ 39 mPa s and $\sim$ 44 mPa s respectively when sheared at 100 s^{-1}. The rheological properties of the inks were tested and coatings were made after 1 day on the RS as well as after 4 days.

Table 4.13: Ink recipe and treatments for investigating the effect of pre-treating ionomer before mixing inks on roller shaker.

Recipe	Ionomer	Alcohol	Dispersion	Treatment	Treatment temperature [°C]
2	A1	NPA	RS 1 day & 4 days	None	-
2	A1	NPA	RS 1 day & 4 days	Heating ionomer and solvent for 1 h prior to mixing	80
2	A1	NPA	RS 1 day & 4 days	Heating ionomer and solvent for 3 h prior to mixing	80

There is no significant difference in the viscosity from being left longer on the RS but the pre-heating does lead to an increased viscosity in the final ink as seen in Figure 4.17. Both moduli are quite low for all samples but they increase with longer treatment times and the G" is higher than G' for most samples which indicates very little elastic buffering as seen in Figure 4.18.

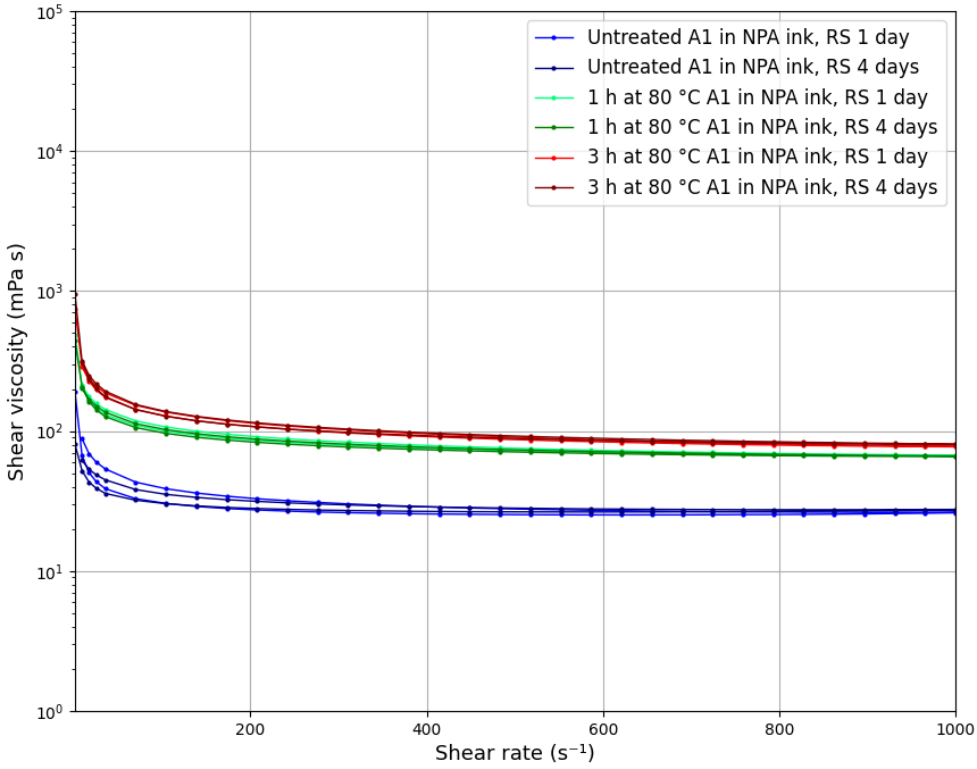

Figure 4.17: Viscosity vs shear rate measurement for inks mixed according to Table 4.13 with NPA as the alcohol. The ink was made with all solvents and ionomer untreated (blue), pre-treated for 1 h at 80 °C (red), and pre-treated for 3 h at 80 °C (green) prior to the ink being mixed. The ink was measured after 1 day and 4 days on RS.

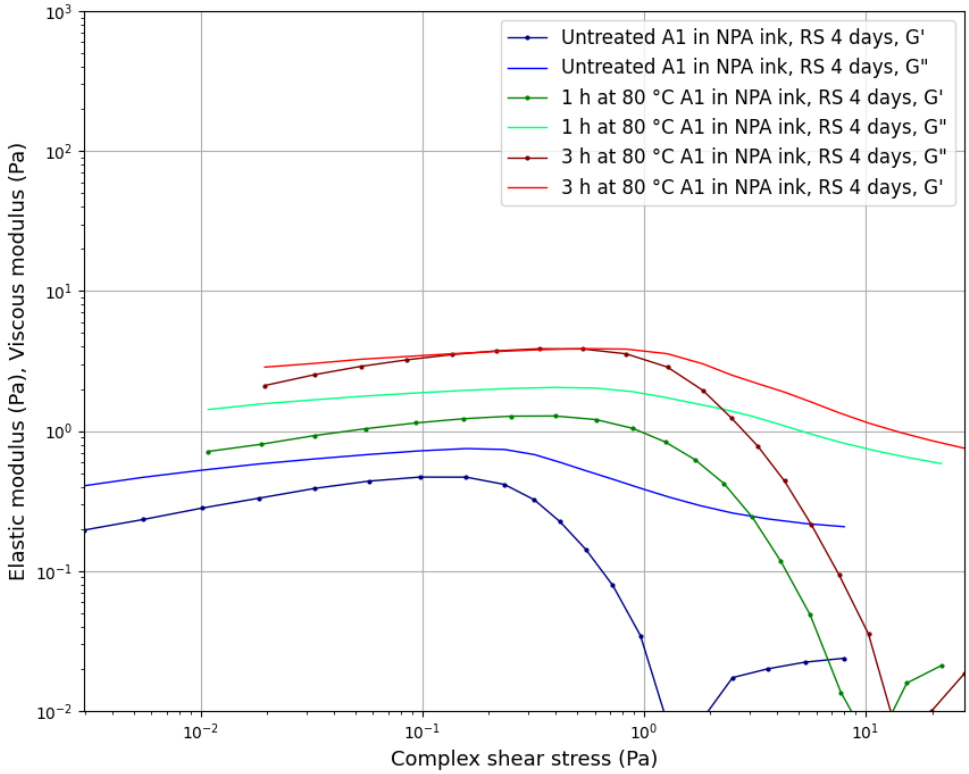

Figure 4.18: Elastic modulus (G') & viscous modulus (G") vs complex shear stress for inks mixed according to Table 4.13 with NPA as the alcohol. The ink was made with all solvents and ionomer untreated (blue), pre-treated for 1 h at 80 °C (red), and pre-treated for 3 h at 80 °C (green) prior to the ink being mixed. The ink was measured after 1 day and 4 days on RS.

Coatings of all three inks were made as well after 1 day and 4 days of mixing. The untreated ink mixed for 1 day dried very unevenly and was full of cracks. After 4 days the coating looks significantly better but there are still spots where the coating cracked and as well as some catalyst powder agglomerates as seen in Figure 4.19 and the microscope pictures in Figure 4.20.

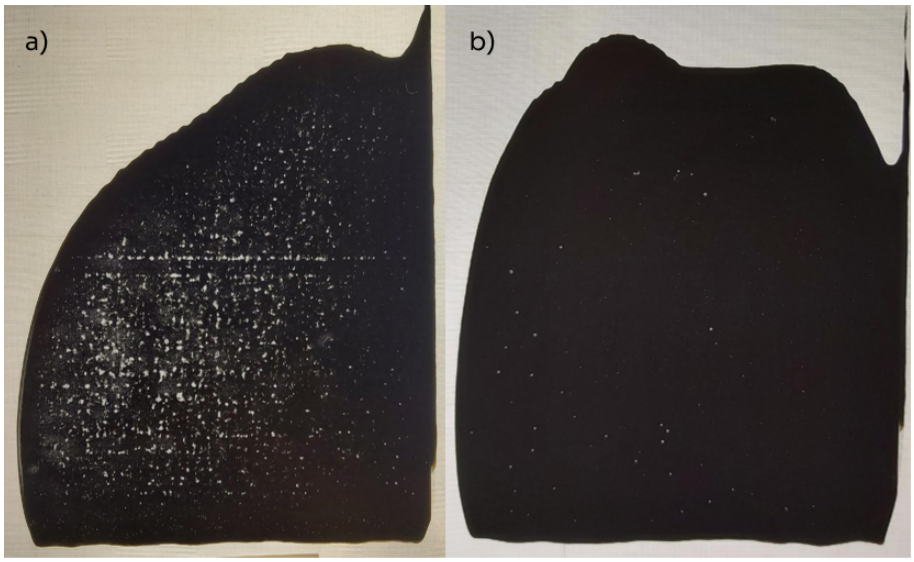

Figure 4.19: Coated decals made from ink with untreated ionomer mixed according to Table 4.13 mixed on the roller shaker. a) is made from ink that has been mixed for 1 day and b) is made from ink that has been mixed for 4 days.

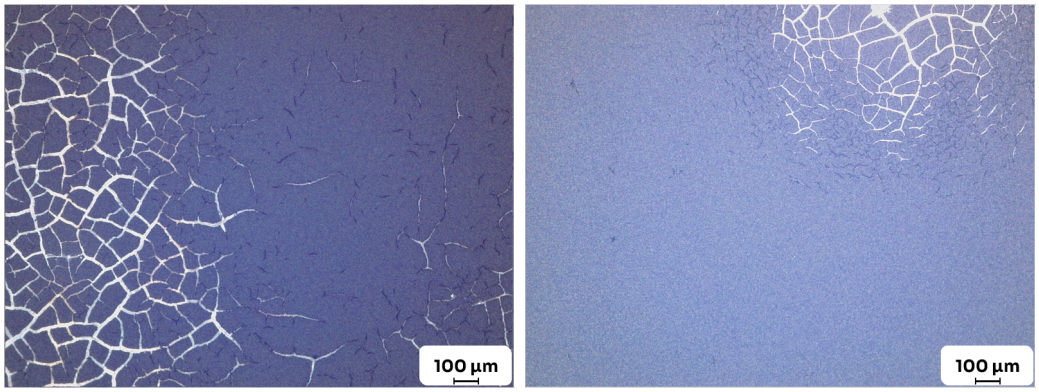

Figure 4.20: Microscope picture of coatings made from untreated ink mixed according to Table 4.13 after 1 day on roller shaker (left) and 4 days on roller shaker (right).

The coatings made from RS ink with pre-treated ionomer look quite different. As can be seen for ink made with ionomer heated for 1 h at 80 °C in Figure 4.21, the bulk of the coating looks very even with hardly any cracks. There are however several large catalyst agglomerates with diameters of ~ 200 μm after 1 day of mixing with cracks around them. After 4 days there are significantly fewer agglomerates and there is less cracking around them. Instead, most agglomerates seem to have split with one large crack across making the agglomerate take the appearance of a coffee bean. These coffee bean agglomerates are ~ 70 μm high.

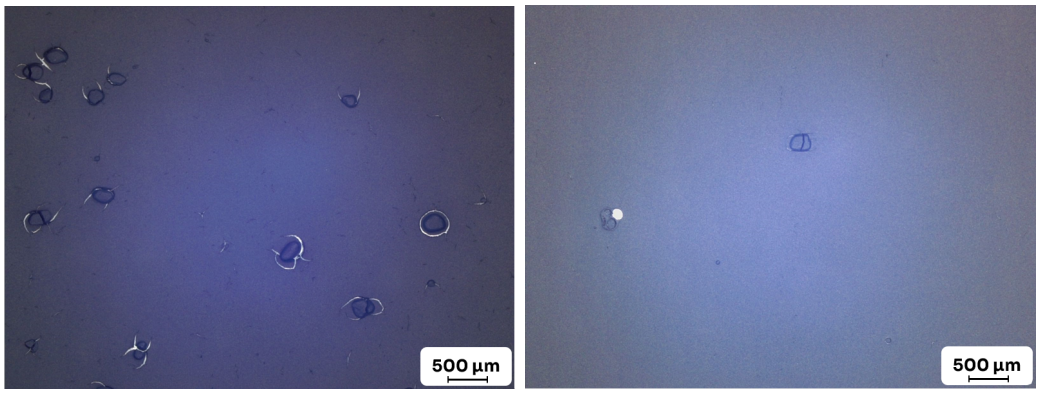

Figure 4.21: Microscope picture of coatings made from ink mixed according to Table 4.13 with ionomer that had been pre-treated for 1 h at 80 °C after 1 day on RS (left) and 4 days on RS (right).

The coatings from ink made with ionomer heated for 3 h at 80 °C seen in Figure 4.22 show the same type of large agglomerates and coffee bean cracks as the 1 h coatings but interestingly there are fewer cracks around the agglomerates making the coating look more opaque. The agglomerates are all around 70 μm or less in height. This is most likely due to the doctor blade having a gap height of 100 μm which means that no agglomerates larger than that could pass under and the agglomerates shrank by around 30 μm when drying. Figure 4.23 shows streaks continuing to be dragged along the backing material after the bulk of the coating stops which suggests that there is a large amount of particles larger than 100 μm in the ink after 1 day of mixing. The 4-day coating does not have these streaks which indicates that fewer and smaller agglomerates are present.

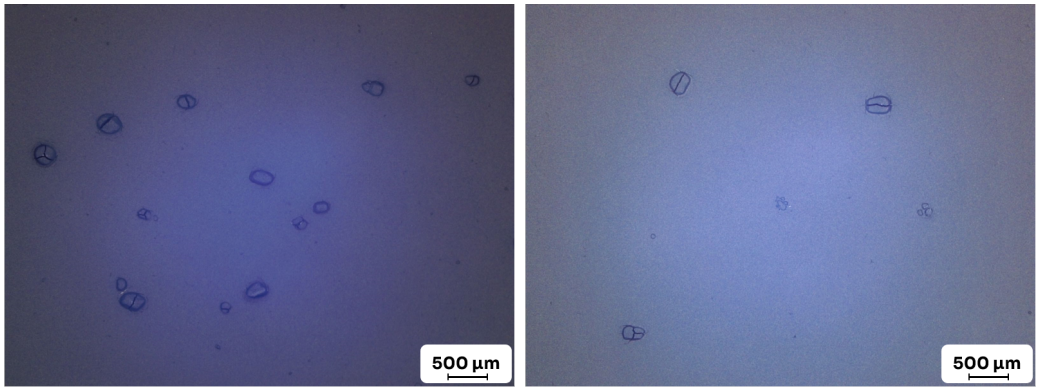

Figure 4.22: Microscope picture of coatings made from ink mixed according to Table 4.13 with ionomer that had been pre-treated for 3 h at 80 °C after 1 day on roller shaker (left) and 4 days on roller shaker (right).

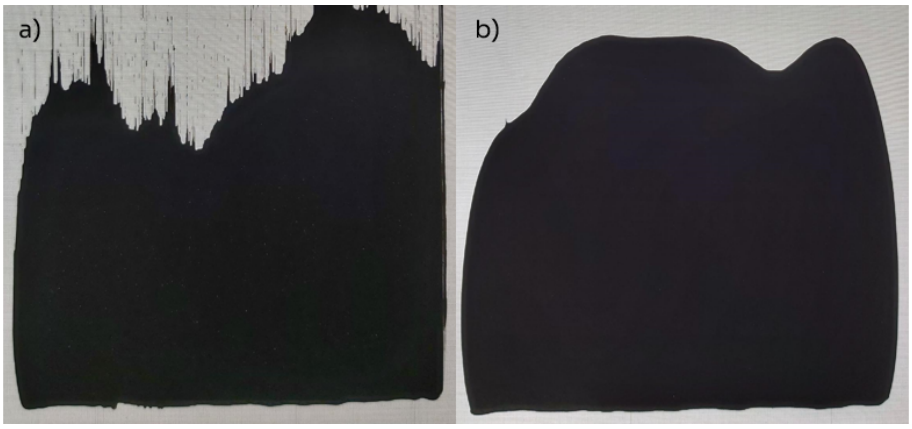

Figure 4.23: Coated decals made from ink mixed according to Table 4.13 mixed on the RS with ionomer that had been pre-treated for 3 h at 80 °C. a) is made from ink that has been mixed for 1 day and b) is made from ink that has been mixed for 4 days.

4.5.2.1 Inks made by conserving solvent for wetting the catalyst

Since there appeared to be still some large lumps in the ink even after 1 days of mixing which had decreased in number but not much in size, a theory with inspiration from cooking was formed. When adding a powder to a liquid like when thickening a sauce with flour or starch, it is common to start by adding the powder to a small amount of liquid first in order to easily break up any clumps and then dilute it with the rest of the liquid. If all of the liquid is added at once, there will form lumps of dry powder which are difficult to get rid of. To see if this sauce theory applies to catalytic inks mixed on the RS, inks with the same 12.6 wt% solid content as above were prepared but instead of adding both the water and the NPA to the ionomer and heating it, the water was instead used to wet the catalyst powder as seen in Table 4.14. The catalyst and water along with three times their total weight of ZrO_2 beads were left to mix on the RS for 1 – 2 h. The ionomer mixture was only heated to 50 °C due to the increased alcohol concentration of 76.14 wt% and the higher ionomer concentration of 5.96 wt%. After 1 h of heating the dispersion had already reached a viscosity of $\sim$ 1000 mPa s when sheared at 100 s^{-1} and displayed a clear shear thinning behavior. After 3 h of heating, the dispersion was very thick and gelatinous with a viscosity of $\sim$ 1400 mPa s when sheared at 100 s^{-1}. This made ink preparation difficult due to the dispersion acting like a solid. The rheological behavior of the inks after 1 day and 7 days of mixing can be seen in Figures 4.24 and 4.25. 7 days of mixing was chosen since the previous batch of inks still had quite a large amount of big agglomerates even after 4 days of mixing. The viscosity decreases with more time on the roller shaker which could be an effect of the ionomer slowly finding an equilibrium state with the additional water and the alcohol that had been trapped in the extended ionomer bundles leaving, causing the bundles to relax. This behavior is not seen if the ionomer is allowed to thicken with all of the solvent present as seen in Subsection 4.5.2.

Table 4.14: Ink recipe and treatments for investigating the effect of pre-treating ionomer and wetting catalyst before mixing inks on roller shaker.

Recipe	**Ionomer**	**Alcohol**	**Dispersion**	**Treatment**	**Treatment temperature [°C]**
2	A1	NPA	RS 1 day & 7 days	Heating ionomer and alcohol for 1 h prior to mixing	50
2	A1	NPA	RS 1 day & 7 days	Heating ionomer and alcohol for 3 h prior to mixing	50

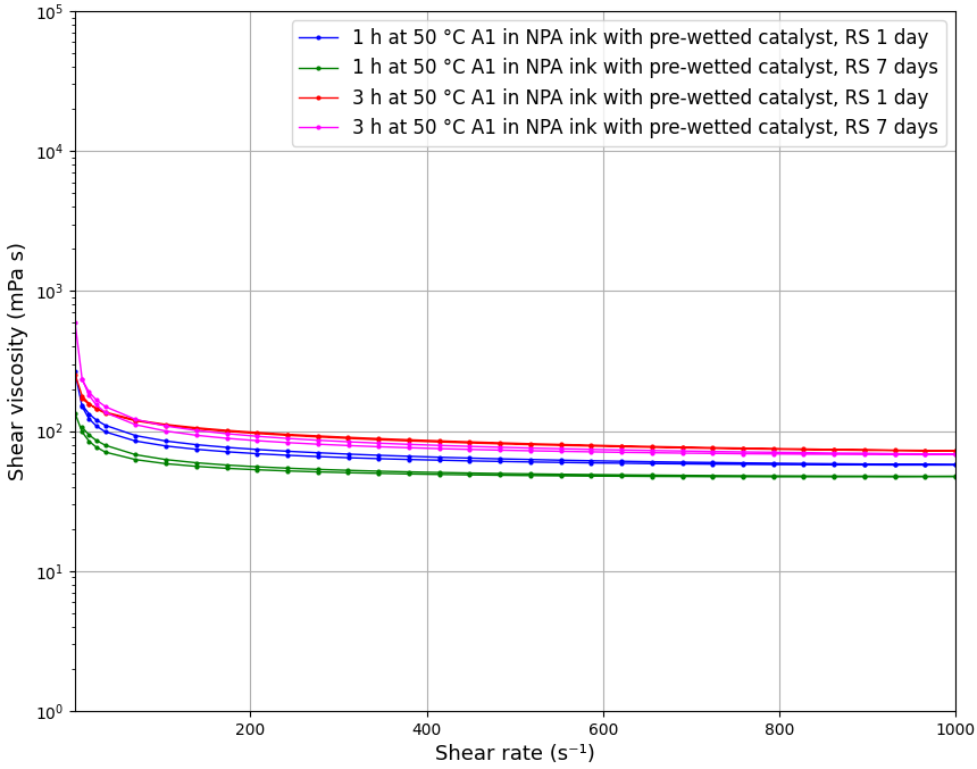

Figure 4.24: Viscosity vs shear rate measurement for inks mixed according to Table 4.14 with pre-wetted catalyst powder, and ionomer and NPA that had been pre-treated for 1 h at 50 °C after 1 day on roller shaker (blue), ionomer and NPA that had been pre-treated for 1 h at 50 °C after 7 days on roller shaker (green), ionomer and NPA that had been pre-treated for 3 h at 50 °C after 1 day on roller shaker (red) and ionomer and NPA that had been pre-treated for 3 h at 50 °C after 7 days on roller shaker (magenta).

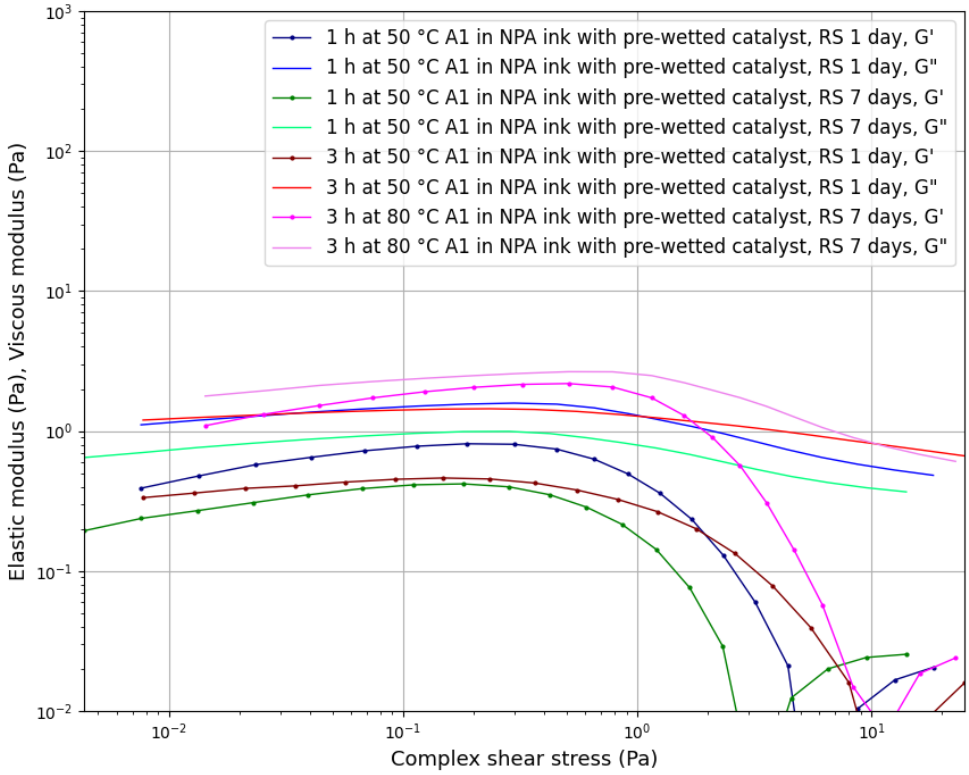

Figure 4.25: Elastic modulus (G') & viscous modulus (G") vs complex shear stress for inks mixed according to Table 4.14 with pre-wetted catalyst powder and ionomer and NPA that had been pre-treated for 1 h at 50 °C after 1 day on roller shaker (blue), ionomer and NPA that had been pre-treated for 1 h at 50 °C after 7 days on roller shaker (green), ionomer and NPA that had been pre-treated for 3 h at 50 °C after 1 day on roller shaker (red) and ionomer and NPA that had been pre-treated for 3 h at 50 °C after 7 days on roller shaker (magenta).

Microscope pictures of coatings made from the inks can be seen in Figure 4.26 and Figure 4.27. Both coatings are full of large agglomerates after 1 day of mixing. The coating made from ink with ionomer pre-treated for 1 h looks similar to coatings from ink without any wetting of the catalyst but the ink made with ionomer pre-treated for 3 h instead has agglomerates with a wide size distribution and generally looks significantly less even. This is most likely due to the ionomer dispersion having completely gelled, causing it to not mix well with the catalyst powder. After 7 days on the RS, both inks give smooth coatings with only a few coffee bean-like agglomerates. There appears to be no clear advantage to pre-wetting the catalyst in this way and it instead causes issues with the preparation.

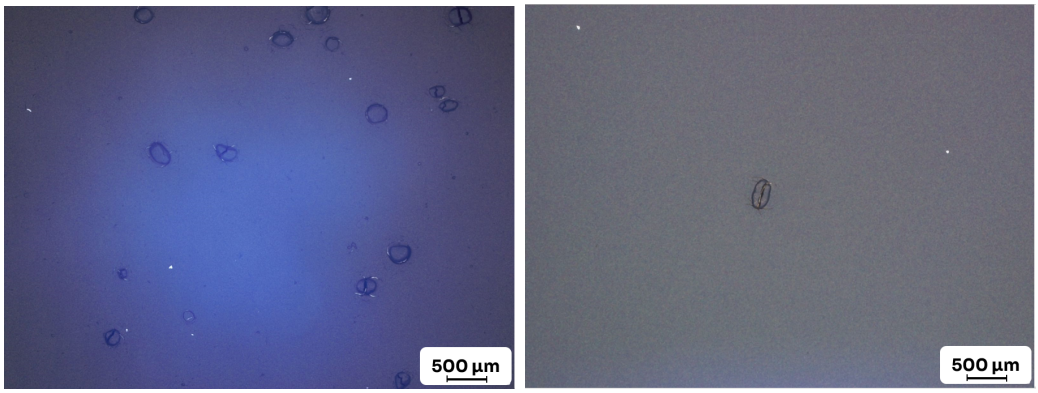

Figure 4.26: Microscope picture of coatings made from ink mixed according to Table 4.14 with ionomer that had been pre-treated for 1 h at 50 °C and pre-wetted catalyst powder after 1 day on roller shaker (left) and 7 days on roller shaker (right).

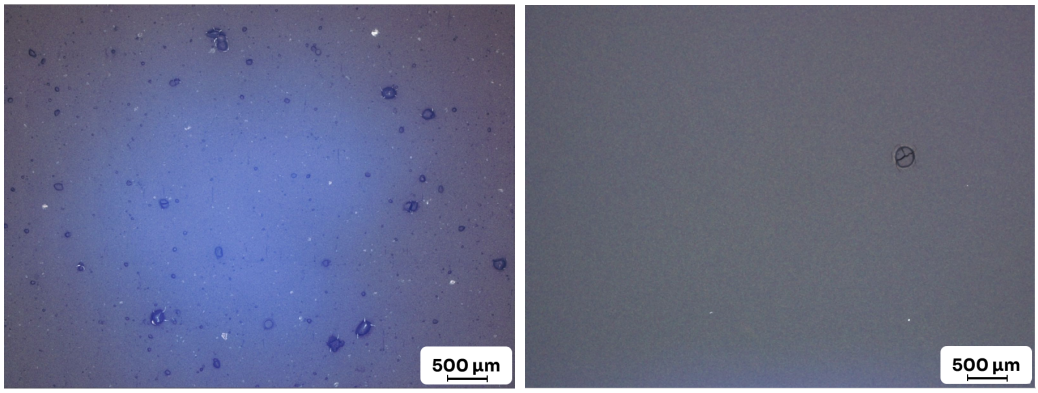

Figure 4.27: Microscope picture of coatings made from ink mixed according to Table 4.14 with ionomer that had been pre-treated for 3 h at 50 °C and pre-wetted catalyst powder after 1 day on roller shaker (left) and 7 days on roller shaker (right).

To explore the theory of pre-wetting the catalyst further, dispersions keeping the 60:40 (w/w) NPA/H_2O with higher ionomer contents of 7 wt% and 10 wt% were made as well and heated at 50 °C for 1 h. The conserved solvent was used to wet the catalyst. For each concentration, one ink was made where the catalyst was allowed to mix on the RS for 1 – 2 h and one where it was allowed to mix overnight. This was done in order to see if more time mixing and grinding of the catalyst powder would help with incorporating the ionomer dispersion. The inks made are described in Table 4.15. These inks were left to mix on the roller shaker for 7 days. There appears to be no major difference in the viscosity or viscoelastic behavior of these inks except that the inks made from the 10 wt% dispersions were slightly thicker. Coatings made from these inks look similar to the ones shown in Figures 4.26 and 4.27.

Table 4.15: Ink recipe and treatments for investigating the effect of pre-treating thicker ionomer dispersions and wetting catalyst before mixing inks on roller shaker.

Recipe	Ionomer	Alcohol	Dispersion	Treatment	Catalyst time on RS	Treatment temperature [°C]
2	A1	NPA	RS 7 days	Heating 7 wt% ionomer dispersion for 1 h prior to mixing	1 - 2 h	50
2	A1	NPA	RS 7 days	Heating 7 wt% ionomer dispersion for 1 h prior to mixing	Overnight	50
2	A1	NPA	RS 7 days	Heating 10 wt% ionomer dispersion for 1 h prior to mixing	1 - 2 h	50
2	A1	NPA	RS 7 days	Heating 10 wt% ionomer dispersion for 1 h prior to mixing	Overnight	50

Interestingly, all four inks made from 7 and 10 wt% ionomer dispersions showed a clear change in rheological behavior during measurement. In the first increasing shearing, the starting viscosity is very high, and a very strong shear thinning behavior is observed at relatively low shear rates. The following decreasing run and the consecutive runs only have a weak shear thinning behavior and the high starting viscosity is not recovered as can be seen in Figure 4.28 which shows one of the inks made from a 10 wt% dispersion. This behavior indicates that the ink had taken on a specific morphology during mixing and loading into the rheometer that was disturbed during shearing and could not be recovered. The ink, therefore, had a different structure after measurement than before. This behavior was not found for any other inks.

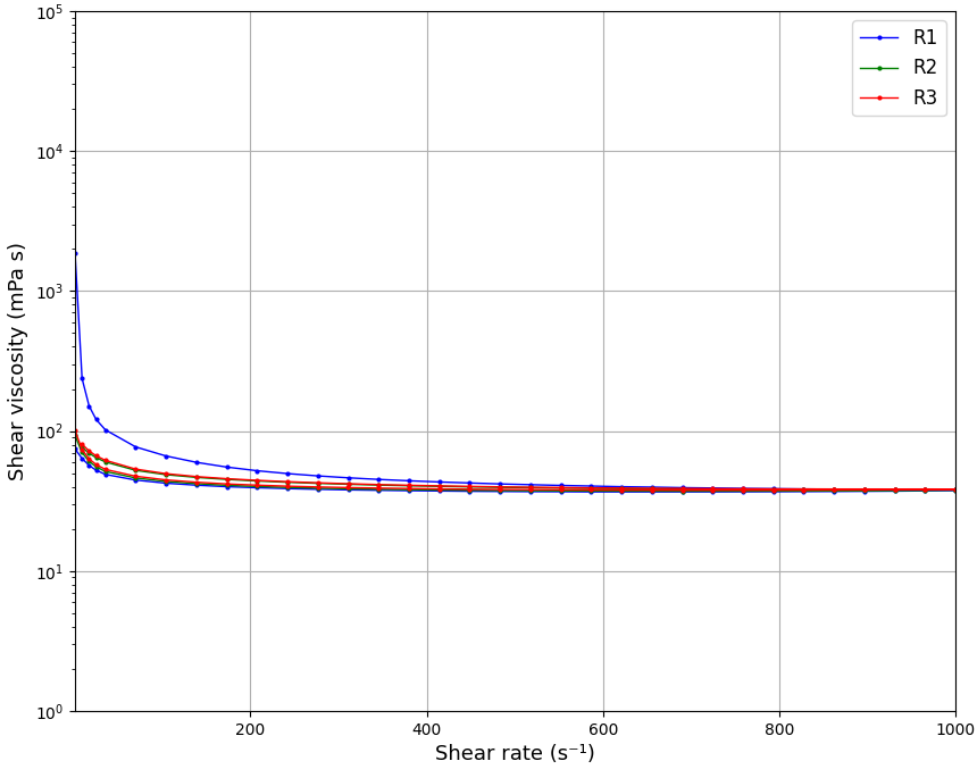

Figure 4.28: Viscosity vs shear rate measurement for ink mixed according to Table 4.15 using NPA as the alcoholic solvent. The ink was made from 10 wt% ionomer dispersion pre-treated for 3 h at 50 °C mixed with a pre-wetted catalyst.

4.5.3 TB based A1 ink

Since TB has a very strong effect on the viscosity of the A1 ionomer before heating, two inks were made according to recipe 2 with a 12.6 wt% solid content as seen in Table 4.16. One ink was mixed with a magnetic stir bar and dispersed with US while the other was allowed to mix on the RS for 1 day and 7 days. The viscosity and viscoelastic behavior of the ink can be found in Figures 4.29 and 4.30.

Table 4.16: Ink recipe and treatments for investigating the effect of TB as a solvent in A1 inks.

Recipe	Ionomer	Alcohol	Dispersion	Treatment
2	A1	TB	US 20 kWs	None
2	A1	TB	RS 1 day & 7 days	None

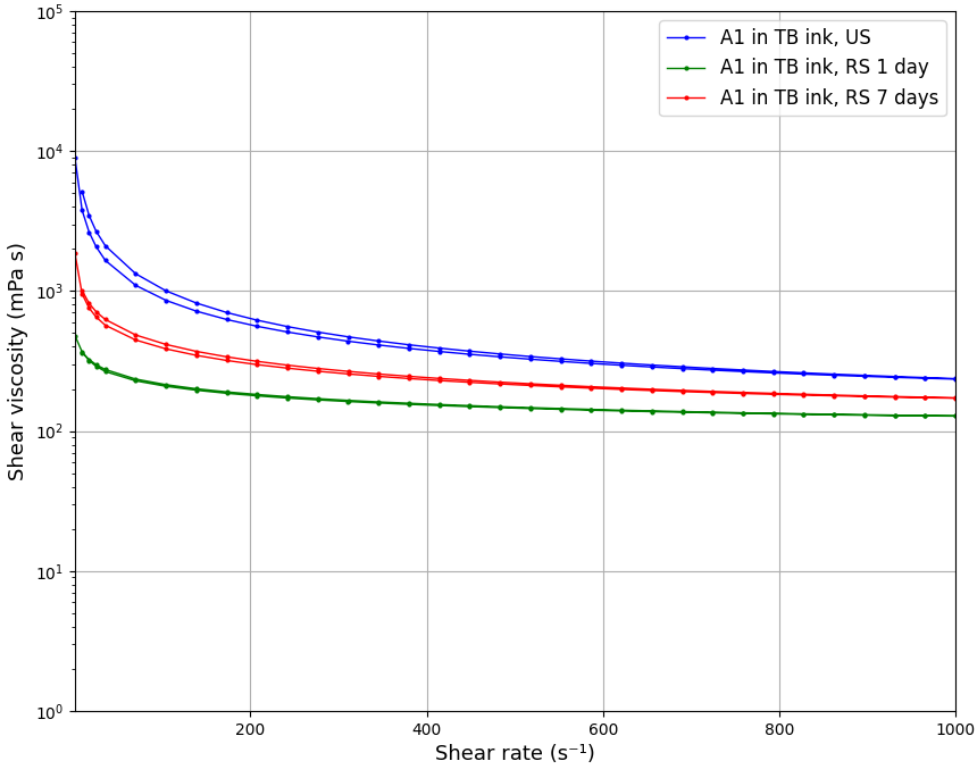

Figure 4.29: Viscosity vs shear rate measurement for inks mixed according to Table 4.16. The ink was dispersed with 20 kWs with US (blue), with RS for 1 day (green), and with RS for 7 days (red).

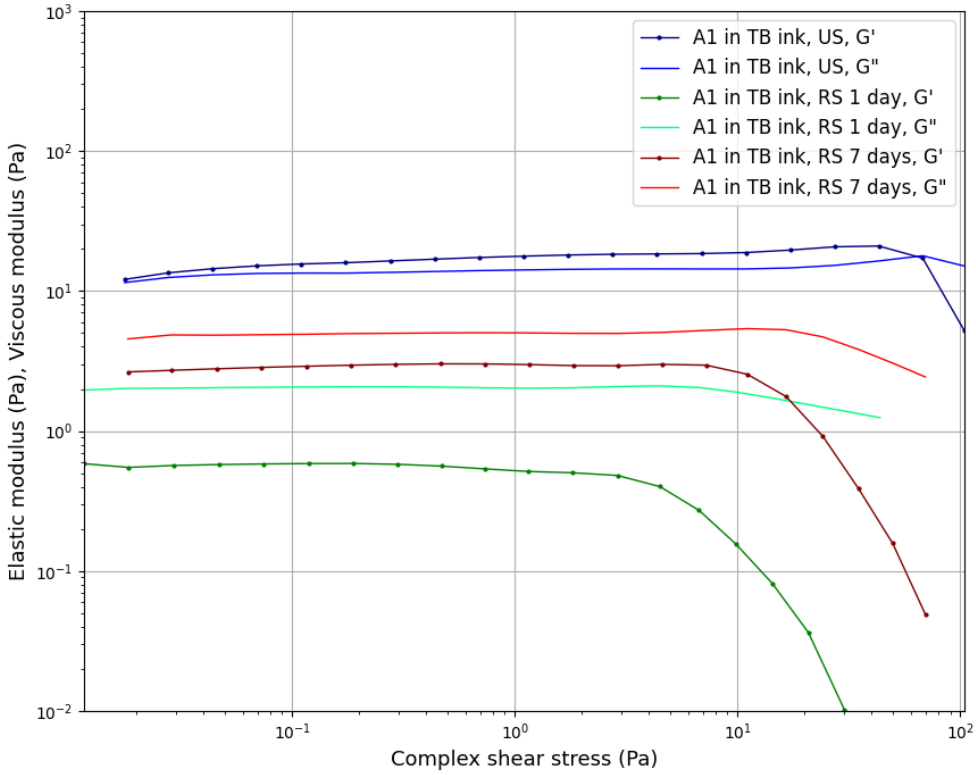

Figure 4.30: Elastic modulus (G') & viscous modulus (G") vs complex shear stress for inks mixed according to Table 4.16. The ink was dispersed with 20 kWs with US (blue), with RS for 1 day (green), and with RS for 7 days (red).

The US ink has a higher viscosity as well as G' and G" than the RS ink which means it is thicker and has more elasticity. The ink was thick enough to start displaying the Weissenberg effect when mixed on the stir plate. Instead of forming a vortex when mixed, the ink formed a "hill" in the middle of the bottle. THis behavior was not observed for any other inks but was seen for some of the very high viscosity ionomer dispersions. The RS ink has a G" which is higher than G' which means that it does not buffer stresses elastically very well. The RS ink was thicker after 7 days of mixing compared to after 1 day which indicates better dispersion of the catalyst as well as more interactions between the ionomer with the catalyst and solvent.

Similarly to the NPA-based inks, the coatings from the ink dispersed with the US had a lot of cracks and several aggregates with a dispersed size range. The largest agglomerates were $\sim$ 30 μm in size as seen in Figure 4.31. The coatings made from ink mixed on with RS instead showed the same smooth bulk as the NPA RS inks with the largest agglomerates being $\sim$ 6 μm. On top of the smooth bulk were large coffee bean cracked agglomerates which were $\sim$ 300 μm in size. Both types of agglomerates can be seen in Figure 4.32. A side-by-side of the two different surfaces can be seen in Figure 4.33. The RS coating made after 7 days looks similar to the

one made after 1 day but with fewer large agglomerates.

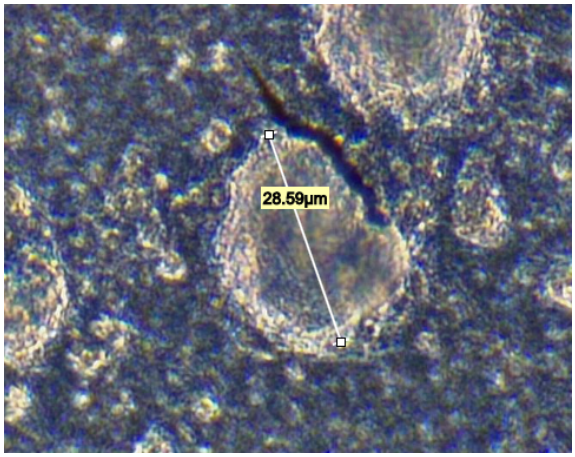

Figure 4.31: Microscopy picture of an agglomerate in a TB-based ink dispersed with US.

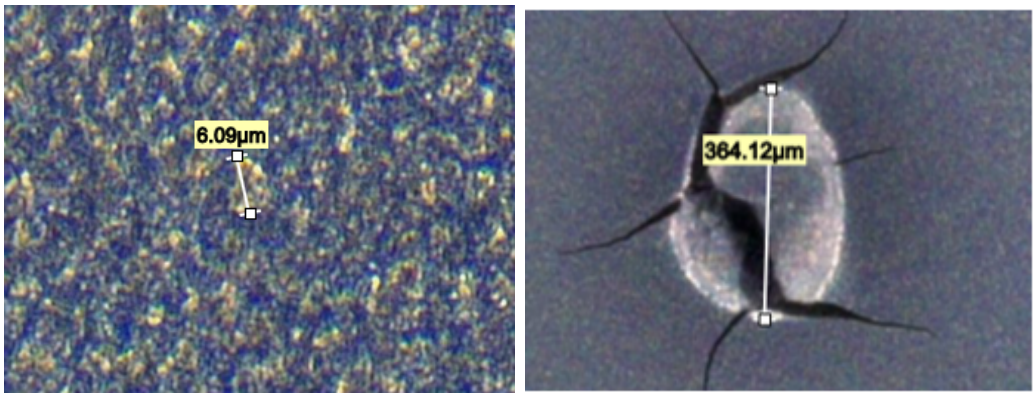

Figure 4.32: Microscopy pictures of an agglomerate found in the bulk of the electrode surface (left) and a larger coffee bean cracked agglomerate (right) in a TB-based ink dispersed with RS for 1 day.

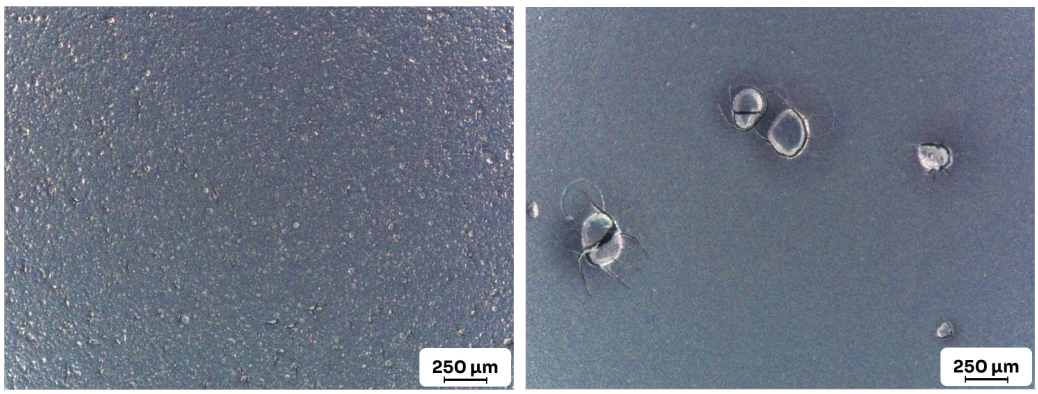

Figure 4.33: Microscopy pictures of in TB-based inks dispersed with US (left) and with RS for 1 day (right).

4.5.3.1 Higher solid content

One ink based on tert-butanol was made according to recipe 1 with a 15.3 wt% solid content and dispersed using US as seen in Table 4.5.3.1. Due to the very strong thickening effect, TB has on the A1 ionomer and the high solid content, the ink completely gelled during the dispersion step and turned into a rubbery solid seen in Figure 4.34. No rheological measurements or coatings could be made from this ink. The heat management was quite poor during the sonication which most likely contributed to the solidification.

Table 4.17: Ink recipe and treatment for investigating the effect of TB as a solvent in A1 inks with higher solid content.

Recipe	Ionomer	Alcohol	Dispersion	Treatment
1	A1	TB	US 20 kWs	None

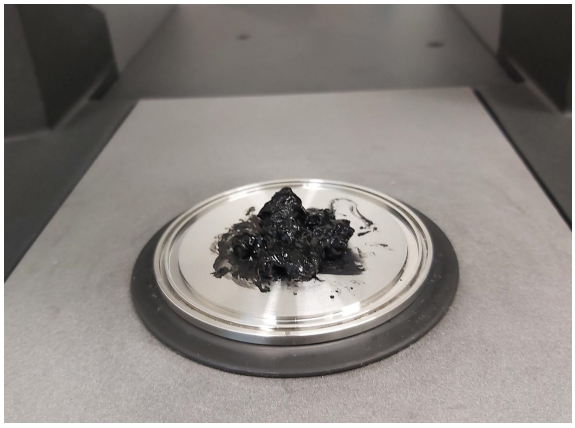

Figure 4.34: Fully solidified tert-butanol and A1 based catalytic ink mixed according to Table 4.5.3.1.

4.5.4 HC based ink

A catalytic ink was made based on the D1 ionomer supplier's recipe with 1.64 wt% ionomer, an I/Pt ratio of 0.39, and a solvent matrix consisting of 50:50 (w/w) IPA/H_2O as seen in recipe 3 in Table 4.10. The ink was mixed and left to mature overnight. The next morning the ink bottle was pressurized and gas appeared to bubble out of solution when it was opened. Due to safety concerns, the bottle was left open if the fume hood and all further tests with D1 ionomer were aborted until the supplier could be contacted. In an interview with supplier D, it became evident that this was an anomaly and not something they had observed before. Due to time constraints, no more investigation was made for this thesis work. Further experiments have been planned at PowerCell.

4.6 Comparison of ink mixing methods

Ultrasonic dispersing has a high instantaneous power input and can therefore ensure that there are no very large agglomerates in the ink but it requires that the ink is thoroughly mixed both beforehand and during the sonication as the sonotrode only affects a very small area. The viscosity will increase up to a certain degree if the ink is heated after mixing and dispersing but this will lead to uneven coatings. Heat management of the ink is very important when using an ionomer that is prone to thicken, especially when the solvent used also promotes thicker inks such as TB.

Inks dispersed on the roller shaker produce more even coatings the longer it is left mixing but even after a full week, there are still large agglomerates. Compared with the US method which can fully disperse an ink in minutes, the RS is not very effective. More ink is also left unrecoverable on the ZrO_2 beads. Ink made with untreated ionomer results in uneven coatings but with fairly small agglomerates. The surface of ink made with pre-thickened ionomer looks very different. The bulk of the electrodes has very small and well-dispersed catalyst aggregates but a significant amount of large agglomerates are also present which trap clumps of catalyst that can not be used in the fuel cell reactions. When drying, these large agglomerates leads to cracks in the surrounding area and/or crack in the characteristic coffee bean way along the middle. The reason behind the formation of the coffee bean-like agglomerates is unknown but it may be that the unfurled ionomer bundles can somehow complex and form stable films that trap lumps of catalyst instead of distributing more evenly as they would when in their micellar state. The unfurling of micelles can either happen when the ionomer is heated or when using a more powerful solvent such as tert-butanol. Conserving some solvent to wet the catalyst powder beforehand does not seem to significantly affect the formation of coffee bean agglomerates. A combination of the US and RS might work well, but this has not been tested.

4.7 Sub-scale MEA tests

An MEA was assembled and tested in-situ from the electrode made from ink with ionomer that had been pre-treated for 1 h at 50 °C and pre-wetted catalyst powder after 7 days on the RS. Figure 4.35 shows the polarization curves for the MEA during normal operating conditions as well as a state-of-the-art in-house MEA from PowerCell.

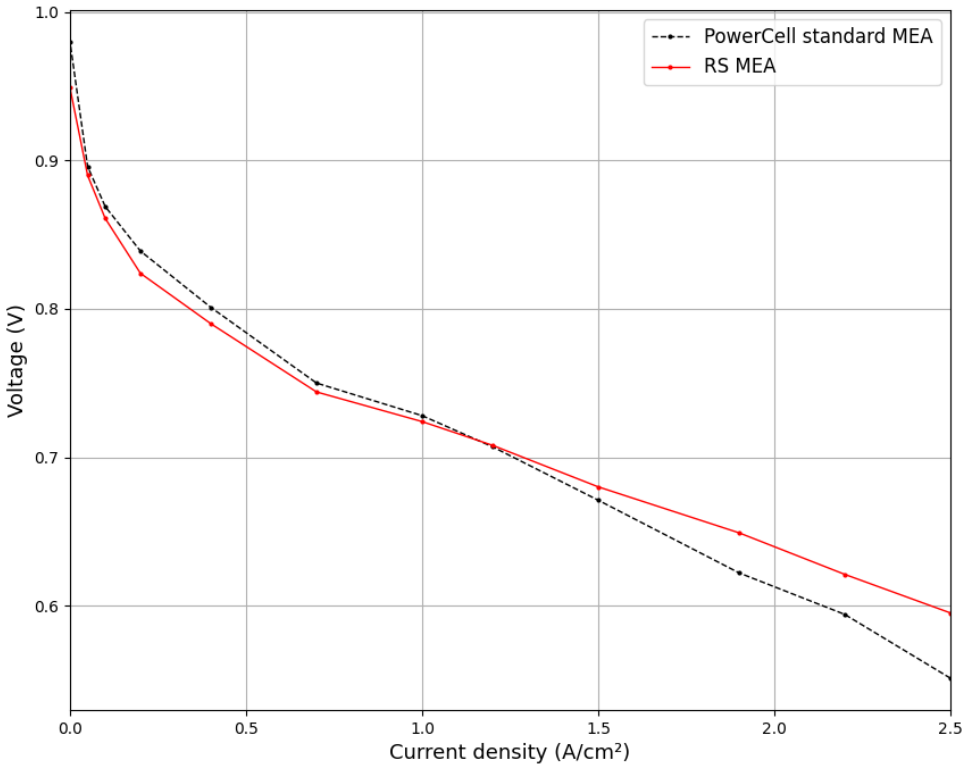

Figure 4.35: Polarization curve showing cell voltage over current density for MEA where cathode ink was made with pre-thickened ionomer and dispersed on the RS for 7 days (red) and a standard in-house produced MEA from PowerCell (black, dashed).

The MEA made with RS ink has a slightly lower open cell voltage than the standard MEA as well as a bit more activation losses in the kinetic region. In the Ohmic region, the voltage losses are $\sim$ 88.5 mV / A/cm^2 compared with $\sim$ 114.6 mV / A/cm^2 for the standard MEA, and this decrease continues linearly up until 2.5 A/cm^2 meaning that there are no significant mass transport losses. The MEA performs fairly well and proves that thickened ionomer dispersions can be mixed with Pt/C on the roller shaker and be used to produce working electrodes. To determine how varying ionomers, solvents, and treatments affect MEA performance, more testing is needed.

5
Conclusion

From Sections 4.1, 4.2 and 4.3 we can conclude that for ionomer A1, higher ionomer concentration, higher alcohol content, and higher temperatures lead to more viscous dispersions. More sterically hindering alcohols give thicker dispersions. Longer treatment times also give higher viscosity but it has less effect than the other parameters and after a certain point which varies depending on the recipe, the dispersion reaches a maximum and will not get any thicker. At this point, the dispersion has turned into a gel. This most likely happens when the ionomer reaches its fully dissolved state where it no longer exists as micelles and all polymer chains are instead extended and entangled with each other. Thicker ionomer dispersions display a stronger shear thinning behavior since the extended polymer chains align themselves with the direction of the shear. To observe this behavior clearly, the ionomer needs to have short-side chains and a low EW. To understand the viscosity dependence of EW and side-chain, more targeted investigation is needed.

Catalytic inks can be made from A1 ionomer that has been pre-treated with certain solvents and temperatures and this affects the structure of the ink as can be seen in both the ink's rheological behavior and in the appearance of the coatings. However, increased viscosity of the components leads to processing issues that need to be resolved before any more thorough investigation of how the ionomer structure interacts with the catalyst and how it affects the performance of the MEAs in-situ. To get a high-viscosity ink when dispersing with the US it is better to use a solvent that interacts more with the ionomer than to thicken up ionomer dispersions beforehand. If the ink is dispersed on the RS, longer mixing times give more even coatings. There are no advantages to pre-wetting the catalyst before adding thickened ionomer dispersions. All RS inks have a very low elastic modulus.

5.1 Outlook

There is an abundance of future research to be made on the ionomer state in catalytic inks. Future topics to investigate include the effect of different solvents on the ionomer in an ink, varying the I/Pt of the ink, and different ionomer interactions with the catalyst in different solvents. There are also many different catalysts that can be used in ink and they would most likely interact differently with the ionomers than the one used in this work. Other ways to investigate the ionomer that might bring more insight than just rheology and microscopy are for example electron microscopy, x-ray and neutron scattering, and quartz crystal microbalance among others. More

sub-scale in-situ testing such as polarization at different operating conditions and cyclic voltammetry would also be helpful if a working, standardized mixing and dispersing method could be established. One suggestion would be to attempt to combine US and RS to eliminate large agglomerates and still ensure adequate mixing. It would in this case be important to differentiate the effects of the ionomer from differences in the processing like the amount of dispersing, maturation times, and drying time which will all be affected by changing any other parameter.

The future will most likely demand more usage of HC ionomers as a replacement for PFSA but seeing as it is not as well developed and understood, more work is needed before it can be used to the same extent. This requiters collaboration between fuel cell manufacturers like PowerCell and the chemical companies developing and selling the ionomers.

Bibliography

[1] William Grove. On Voltic Series and the Combination of Gases by Platinum. *The London, Edinburgh, and Dublin Philosophical Magazine and Journal of Science*, 14(86):127–130, 1839.

[2] William Grove. On a Gaseous Voltaic Battery. *The London, Edinburgh, and Dublin Philosophical Magazine and Journal of Science*, 21(140):417–420, 1842.

[3] Frano Barbir. *PEM Fuel Cells - Theory and Practice.* Academic Press, Waltham, MA, 2nd ed. edition, 2013. ISBN 9780123877109.

[4] PowerCell Group. Hydrogen Fuel Cells, 2023. URL `https://powercellgroup.com/hydrogen-fuel-cell/`.

[5] Klaus-Dieter Kreuer. *Fuel Cells.* ISBN 978-1-4614-5784-8. doi: 10.1007/978-1-4614-5785-5.

[6] Jennifer Peron, Zhiqing Shi, and Steven Holdcroft. Hydrocarbon proton conducting polymers for fuel cell catalyst layers. *Energy and Environmental Science*, 4(5):1575–1591, 5 2011. doi: 10.1039/c0ee00638f.

[7] Steven Holdcroft. Fuel cell catalyst layers: A polymer science perspective, 1 2014.

[8] Tobias Morawietz, Michael Handl, Claudio Oldani, K. Andreas Friedrich, and Renate Hiesgen. Quantitative in Situ Analysis of Ionomer Structure in Fuel Cell Catalytic Layers. *ACS Applied Materials and Interfaces*, 8(40):27044–27054, 10 2016. doi: 10.1021/acsami.6b07188.

[9] Nagappan Ramaswamy, Swami Kumaraguru, Roland Koestner, Timothy Fuller, Wenbin Gu, Nancy Kariuki, Deborah Myers, Peter J. Dudenas, and Ahmet Kusoglu. Editors' Choice—Ionomer Side Chain Length and Equivalent Weight Impact on High Current Density Transport Resistances in PEMFC Cathodes. *Journal of The Electrochemical Society*, 168(2):024518, 2 2021. doi: 10.1149/1945-7111/abe5eb.

[10] Tobias Morawietz, Michael Handl, Kaspar Andreas Friedrich, and Renate Hiesgen. Structure, Properties, and Degradation of Ultrathin Ionomer Films in Catalytic Layers of Fuel Cells. *ECS Transactions*, 86(13):179–191, 7 2018. doi: 10.1149/08613.0179ecst.

[11] Jong Hyeok Park, Mun Sik Shin, and Jin Soo Park. Effect of dispersing solvents for ionomers on the performance and durability of catalyst layers in proton

exchange membrane fuel cells. *Electrochimica Acta*, 391, 9 2021. doi: 10.1016/j.electacta.2021.138971.

[12] Ji Hye Lee, Gisu Doo, Sung Hyun Kwon, Sungyu Choi, Hee Tak Kim, and Seung Geol Lee. Dispersion-Solvent Control of Ionomer Aggregation in a Polymer Electrolyte Membrane Fuel Cell. *Scientific Reports*, 8(1), 12 2018. doi: 10.1038/s41598-018-28779-y.

[13] Jian Xie, Fan Xu, David L. Wood, Karren L. More, Thomas A. Zawodzinski, and Wayne H. Smith. Influence of ionomer content on the structure and performance of PEFC membrane electrode assemblies. *Electrochimica Acta*, 55(24): 7404–7412, 10 2010. doi: 10.1016/j.electacta.2010.06.067.

[14] Apichai Therdthianwong, Panuwat Ekdharmasuit, and Supaporn Therdthianwong. Fabrication and performance of membrane electrode assembly prepared by a catalyst-coated membrane method: Effect of solvents used in a catalyst ink mixture. *Energy and Fuels*, 24(2):1191–1196, 2 2010. doi: 10.1021/ef901105k.

[15] Irene Gatto, Ada Saccà, David Sebastián, Vincenzo Baglio, Antonino Salvatore Aricò, Claudio Oldani, Luca Merlo, and Alessandra Carbone. Influence of Ionomer content in the catalytic layer of MEAS based on aquivion® Ionomer. *Polymers*, 13(21), 11 2021. doi: 10.3390/polym13213832.

[16] R. M. Rioux and M. A. Vannice. Dehydrogenation of isopropyl alcohol on carbon-supported Pt and Cu–Pt catalysts. *Journal of Catalysis*, 233(1):147–165, 7 2005. doi: 10.1016/J.JCAT.2005.04.020.

[17] Shaojie Du, Wenkang Li, Han Wu, Po Ya Abel Chuang, Mu Pan, and Pang Chieh Sui. Effects of ionomer and dispersion methods on rheological behavior of proton exchange membrane fuel cell catalyst layer ink. *International Journal of Hydrogen Energy*, 45(53):29430–29441, 10 2020. doi: 10.1016/j.ijhydene.2020.07.241.

[18] Ahmet Kusoglu and Adam Z. Weber. New Insights into Perfluorinated Sulfonic-Acid Ionomers. *Chemical Reviews*, 117(3):987–1104, 2 2017. doi: 10.1021/acs.chemrev.6b00159.

[19] Chen Wang, Veena Krishnan, Dongsheng Wu, Rylan Bledsoe, Stephen J. Paddison, and Gerd Duscher. Evaluation of the microstructure of dry and hydrated perfluorosulfonic acid ionomers: Microscopy and simulations. *Journal of Materials Chemistry A*, 1(3):938–944, 1 2013. doi: 10.1039/c2ta01034h.

[20] Ali Malek, Ehsan Sadeghi, Jasna Jankovic, Michael Eikerling, and Kourosh Malek. Aquivion Ionomer in Mixed Alcohol–Water Solution: Insights from Multiscale Molecular Modeling. *The Journal of Physical Chemistry C*, 124(6): 3429–3438, 2 2020. doi: 10.1021/acs.jpcc.9b08969.

[21] Deborah Jones. Perfluorosulfonic Acid Membranes for Fuel Cell and Electrolyser Applications. *Material Matters*, 10(3):88–92, 2015.

[22] Ting Li, Jiabin Shen, Guangying Chen, Shaoyun Guo, and Guangyou Xie. Performance Comparison of Proton Exchange Membrane Fuel Cells with Nafion

and Aquivion Perfluorosulfonic Acids with Different Equivalent Weights as the Electrode Binders. *ACS Omega*, 5(28):17628–17636, 7 2020. doi: 10.1021/acsomega.0c02110.

[23] Dennis E. Curtin, Robert D. Lousenberg, Timothy J. Henry, Paul C. Tangeman, and Monica E. Tisack. Advanced materials for improved PEMFC performance and life. *Journal of Power Sources*, 131(1-2):41–48, 5 2004. doi: 10.1016/j.jpowsour.2004.01.023.

[24] L. Ghassemzadeh, K. D. Kreuer, J. Maier, and K. Müller. Evaluating chemical degradation of proton conducting perfluorosulfonic acid ionomers in a Fenton test by solid-state 19F NMR spectroscopy. *Journal of Power Sources*, 196(5):2490–2497, 3 2011. doi: 10.1016/j.jpowsour.2010.11.053.

[25] Benoit Loppinet and Gérard Gebel. Rodlike Colloidal Structure of Short Pendant Chain Perfluorinated Ionomer Solutions. *Langmuir*, 14(8):1977–1983, 1998.

[26] Kenneth A. Mauritz and Robert B. Moore. State of understanding of Nafion. *Chemical Reviews*, 104(10):4535–4585, 10 2004. doi: 10.1021/cr0207123.

[27] Cynthia Welch, Andrea Labouriau, Rex Hjelm, Bruce Orler, Christina Johnston, and Yu Seung Kim. Nafion in dilute solvent systems: Dispersion or solution? *ACS Macro Letters*, 1(12):1403–1407, 12 2012. doi: 10.1021/mz3005204.

[28] Swedish Chemical Agency. PFAS, 5 2023. URL `https://www.kemi.se/en/chemical-substances-and-materials/pfas#h-WhatarePFAS`.

[29] European Chemical Agency. ECHA publishes PFAS restriction proposal, 2 2023. URL `https://echa.europa.eu/sv/-/echa-publishes-pfas-restriction-proposal`.

[30] 3M. 3M to Exit PFAS Manufacturing by the End of 2025, 12 2022. URL `https://news.3m.com/2022-12-20-3M-to-Exit-PFAS-Manufacturing-by-the-End-of-2025`.

[31] Xingtong Pu, Yuting Duan, Jialin Li, Chunyu Ru, and Chengji Zhao. Understanding of hydrocarbon ionomers in catalyst layers for enhancing the performance and durability of proton exchange membrane fuel cells. *Journal of Power Sources*, 493, 5 2021. doi: 10.1016/j.jpowsour.2021.229671.

[32] Hien Nguyen, Florian Lombeck, Claudia Schwarz, Philipp A. Heizmann, Michael Adamski, Hsu Feng Lee, Benjamin Britton, Steven Holdcroft, Severin Vierrath, and Matthias Breitwieser. Hydrocarbon-based Pemion™ proton exchange membrane fuel cells with state-of-the-art performance. *Sustainable Energy and Fuels*, 5(14):3687–3699, 7 2021. doi: 10.1039/d1se00556a.

[33] Michael Adamski, Thomas J. G. Skalski, Benjamin Britton, Timothy J. Peckham, Lukas Metzler, and Steven Holdcroft. Highly Stable, Low Gas Crossover, Proton-Conducting Phenylated Polyphenylenes. *Angewandte Chemie*, 129(31):9186–9189, 7 2017. doi: 10.1002/ange.201703916.

[34] Netzsch. A Basic Introduction to Rheology. Technical report. URL www.netzsch.com.

DEPARTMENT OF PHYSICS
CHALMERS UNIVERSITY OF TECHNOLOGY
Gothenburg, Sweden
www.chalmers.se

CHALMERS
UNIVERSITY OF TECHNOLOGY